Schweizerische Eidgenossenschaft
Confédération suisse
Confederazione Svizzera
Confederaziun svizra

Department of the Environment,
Transport, Energy and Communication DETEC

**Swiss Federal Office of Energy SFOE**
Energy Research and Cleantech

**Final report**

# Power system protection in presence of high shares of distributed converter-interfaced resources

PRODICON

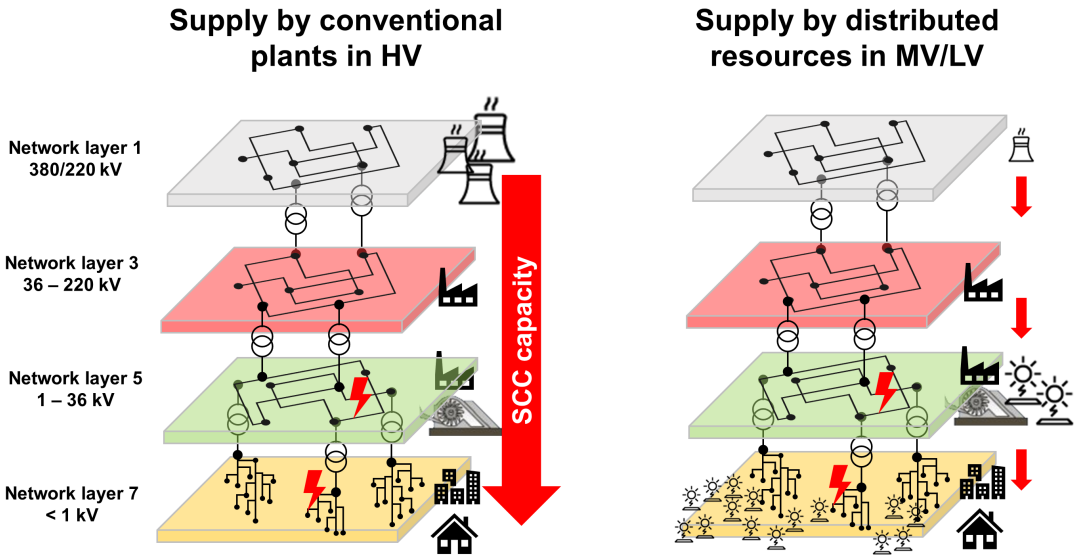

RESEARCH CENTER FOR ENERGY NETWORKS
FORSCHUNGSSTELLE ENERGIENETZE

**Date:** 08. August 2024

**Place:** Bern

**Publisher:**
Swiss Federal Office of Energy SFOE
Research Programme Grids
CH-3003 Bern
www.bfe.admin.ch
energieforschung@bfe.admin.ch

**Subsidy rescipient:**
ETH Zürich
Forschungsstelle Energienetze (FEN)
Sonneggstrasse 28,CH-8092 Zürich
www.fen.ethz.ch

**Authors:**
Cansin Yaman Evrenosoglu, Forschungsstelle Energienetze - ETH Zürich, evrenos@fen.ethz.ch
Turhan Demiray, Forschungsstelle Energienetze - ETH Zürich, demirayt@fen.ethz.ch
Alexander Fuchs, Forschungsstelle Energienetze - ETH Zürich, fuchs@fen.ethz.ch

**SFOE project coordinator:** Dr. Michael Moser, michael.moser@bfe.admin.ch
**SFOE contract number:** SI/502101-01

## Summary

The objectives of this project are (i) to analyze the impacts of converter-interfaced resources in distribution grids on the protection layouts of medium- and low-voltage distribution grids (MV and LV) and (ii) to assess the efficacy of the state-of-the-art methods for designing and assessing the protection layouts in distribution grids by using a quantitative framework: For (i) the focus is given to the future generation layouts when the number of conventional generators at high voltage (HV) and extra-high voltage (EHV) grids are varying significantly daily (e.g., summer daytime) and seasonally (e.g., summer vs. winter). For example, distributed generation at MV and LV grids such as solar PVs are expected to supply most of the demand on summer days. Since the number of online rotating machines at HV and EHV grids is reduced, maximum short-circuit currents (Ik") supplied by the HV and EHV grids to the faults in the MV and LV grids are expected to significantly reduce, will result in not activation or delayed activation of the protection devices. This phenomenon is known as "*protection under-reach*", and not desired by the grid operators. In addition, due to the short-circuit current contribution of distributed generation at MV- and LV-grids, unnecessary activation of protection devices in feeders without faults are expected, especially if the protection devices are non-directional. This phenomenon is known as "*nuisance & sympathetic tripping*", and not desired by the operators, either. For (ii), the industrial standard, IEC60909-2016, which is widely used in the industry when designing and assessing the distribution grid protection systems, is assessed by using the results of the RMS simulations for selected generation layouts in (i).

In this report, first the benefits of RMS simulations (compared to the results of the IEC60909-2016 standard) for protection studies are demonstrated, especially when the grid voltages are deviating significantly from nominal voltage. For RMS simulations, the FEN in-house tool, FlexDYN*, is used. Next, the fault levels (i.e., short-circuit current levels, Ik") in a given MV grid for selected grid operating states with high and low renewable energy resources such as PV is assessed. Following, the impacts of different fault levels in selected grid operating states on overcurrent protection of MV-LV transformers and MV cables as well as back-up protection are demonstrated, and finally a non-exhaustive list of potential mitigation measures is provided. For simulations and analyses, an MV grid is used, shared by EKZ in PowerFactory format, including MV-LV transformers, while the LV loads are aggregated at the LV side of the transformers.

The analysis shows that it is essential to consider the time-variant short circuit current (i.e., fault level, $S_k^{''}$) contribution from upper grids, projected for 2035+ when the number of spinning generators will be lower in ENTSO-E region. In extreme cases, for example when $S_k^{''}$ is 10% or less than today's values, the use of the IEC60909-2016 standard in assessing the functionalities of the protection devices lead to inaccurate results. Depending on the location of the LV bus (i.e., proximity to HV-MV transformer), the MV-LV transformer's characteristics, and the location of the PVs (i.e., at MV vs. LV), IEC60909-2016 may significantly underestimate or overestimate the fault levels at the LV bus. The undesired phenomena such as protection under-reach and nuisance & sympathetic tripping during short circuits in MV and LV grids are detected and better observed by using RMS simulations, especially when $S_k^{''}$ from upper grids is significantly lower. Due to short-circuit current contribution of solar PVs, the protection back-up coordination for overcurrent protection of cables are expected to be severely affected. The short-circuit current levels at the LV side of the transformers are expected to be affected. If the utility uses HHS (Hochspannungs-Hochleistungs-Sicherung / HV-fuse) in coordination with the protection devices at the LV feeders, the coordination settings shall be re-assessed for different operating conditions (e.g., high PV generation with low $S_k^{''}$).


*https://www.fen.ethz.ch/activities/tools/flexdyn.html

# Zusammenfassung

Die Ziele dieses Projekts sind (i) die Analyse der Auswirkungen von umrichtergekoppelten Ressourcen auf die Schutzkonzepte von Mittel- und Niederspannungsnetzen (MS und NS) und (ii) die Bewertung der Wirksamkeit der derzeitigen Methoden für den Entwurf und die Bewertung von Schutzkonzepten in Verteilungsnetzen unter Verwendung eines quantitativen Rahmens: Bei (i) liegt der Schwerpunkt auf den zukünftigen Erzeugungsauslegungen, wenn die Anzahl der konventionellen Erzeuger in Hoch- und Höchstspannungsnetzen täglich (z. B. im Sommer tagsüber) und saisonal (z. B. im Sommer und im Winter) stark schwankt. So wird beispielsweise erwartet, dass die dezentrale Erzeugung in den Mittel- und Niederspannungsnetzen, z. B. durch Photovoltaikanlagen, den größten Teil der Nachfrage an Sommertagen deckt. Da die Anzahl der online geschalteten rotierenden Maschinen in Hoch- und Höchstspannungsnetzen reduziert ist, wird erwartet, dass die maximalen Kurzschlussströme (Ik"), die von den Hoch- und Höchstspannungsnetzen zu den Fehlern in den Mittel- und Niederspannungsnetzen geliefert werden, deutlich sinken, was dazu führt, dass die Schutzeinrichtungen nicht oder erst später aktiviert werden. Dieses Phänomen wird als "Schutzunterdeckung" bezeichnet und ist von den Netzbetreibern nicht erwünscht. Darüber hinaus ist aufgrund des Kurzschlussstrombeitrags der dezentralen Erzeugung in den Mittel- und Niederspannungsnetzen mit einer unnötigen Auslösung von Schutzeinrichtungen in den nachgeschalteten Abgängen der Umspannwerke ohne Fehler zu rechnen, insbesondere wenn die Schutzeinrichtungen nicht richtungsabhängig sind. Dieses Phänomen ist als "störende & sympathetische Auslösung" bekannt und von den Betreibern auch nicht erwünscht. Für (ii) wird die Industrienorm IEC60909-2016, die in der Industrie bei der Auslegung und Bewertung von Schutzsystemen für Verteilungsnetze weit verbreitet ist, anhand der Ergebnisse der RMS-Simulationen für ausgewählte Erzeugungslayouts in (i) bewertet.

In diesem Bericht wird zunächst der Nutzen von RMS-Simulationen (im Vergleich zu den Ergebnissen der Norm IEC60909-2016) für Schutzstudien aufgezeigt, insbesondere wenn die Netzspannungen erheblich von der Nennspannung abweichen. Als Nächstes werden die Fehlerniveaus (d. h. Kurzschlussstromniveaus, Ik") in einem gegebenen Mittelspannungsnetz für ausgewählte Netzbetriebszustände mit hohen und niedrigen erneuerbaren Energieressourcen wie PV bewertet. Anschließend werden die Auswirkungen verschiedener Fehlerpegel in ausgewählten Netzbetriebszuständen auf den Überstromschutz von MV-LV-Transformatoren und MV-Kabeln sowie auf den Reserveschutz aufgezeigt, und schließlich wird eine nicht erschöpfende Liste potenzieller Abhilfemaßnahmen vorgelegt. Für die Simulationen und Analysen wird ein von EKZ geteiltes MS-Netz im PowerFactory-Format mit MS-NS-Transformatoren verwendet, während die NS-Lasten auf der NS-Seite der Transformatoren aggregiert werden (ohne NS-Netze).

Die Analyse zeigt, dass es wichtig ist, den zeitvariablen Kurzschlussstrombeitrag (d. h. den Fehlerpegel $S_k^{''}$) der oberen Netze zu berücksichtigen, der für das Jahr 2035+ prognostiziert wird, wenn die Anzahl der sich drehenden Generatoren im ENTSO-E Gebiet geringer sein wird. In extremen Fällen, z.B. wenn $S_k^{''}$ 10% oder weniger als die heutigen Werte beträgt, führt die Verwendung der Norm IEC60909-2016 bei der Bewertung der Funktionalitäten der Schutzeinrichtungen zu ungenauen Ergebnissen. Je nach Lage der NS-Sammelschiene (d. h. in der Nähe des MS-MS-Transformators), den Eigenschaften des MS-NS-Transformators und der Lage der PV-Anlagen (d. h. auf MS- oder NS-Ebene) kann die IEC60909-2016 die Fehlerpegel auf der NS-Sammelschiene erheblich unterschätzen oder überschätzen. Unerwünschte Phänomene wie Schutzunterschreitungen und unerwünschte Auslösungen während Kurzschlüssen in Mittel- und Niederspannungsnetzen werden durch die Verwendung von RMS-Simulationen erkannt und besser beobachtet, insbesondere wenn $S_k^{''}$ aus den oberen Netzen deutlich niedriger ist. Aufgrund des Kurzschlussstrombeitrags von PV-Anlagen wird erwartet, dass die Schutz-Backup-Koordination für den Überstromschutz von Kabeln stark beeinträchtigt wird. Es wird erwartet, dass die Kurzschlussstrompegel auf der Niederspannungsseite der Transformatoren beeinträchtigt werden. Wenn das Energieversorgungsunternehmen HHS (Hochspannung-Hochleistung Sicherung) in Koordination mit den Schutzeinrichtungen an den NS-Abgängen einsetzt, müssen die Koordinationseinstellungen für unterschiedliche Betriebsbedingungen (z. B. hohe PV-Erzeugung mit niedrigem $S_k^{''}$) neu bewertet werden.

# Résumé

Les objectifs de ce projet sont (i) d'analyser les impacts des ressources interfacées avec les convertisseurs dans les réseaux de distribution sur les schémas de protection des réseaux de distribution moyenne et basse tension (MV et LV) et (ii) d'évaluer l'efficacité des méthodes de pointe pour la conception et l'évaluation des schémas de protection dans les réseaux de distribution à l'aide d'un cadre quantitatif : Pour (i), l'accent est mis sur les futurs schémas de production lorsque le nombre de générateurs conventionnels sur les réseaux à haute tension (HT) et à très haute tension (THT) varie considérablement d'un jour à l'autre (par exemple, pendant la journée en été) et d'une saison à l'autre (par exemple, en été et en hiver). Par exemple, la production distribuée sur les réseaux MT et BT, telle que les panneaux solaires photovoltaïques, est supposée répondre à la majeure partie de la demande les jours d'été. Étant donné que le nombre de machines rotatives en ligne sur les réseaux HT et THT est réduit, les courants de court-circuit maximaux (Ik") fournis par les réseaux HT et THT aux défauts sur les réseaux MT et BT devraient diminuer de manière significative, ce qui entraînera la non-activation ou l'activation retardée des dispositifs de protection. Ce phénomène, connu sous le nom de « protection under-reach », n'est pas souhaité par les gestionnaires de réseau. En outre, en raison de la contribution du courant de court-circuit de la production distribuée aux réseaux MT et BT, on peut s'attendre à une activation inutile des dispositifs de protection dans les lignes d'alimentation sans défaut, en particulier si les dispositifs de protection ne sont pas directionnels. Ce phénomène est connu sous le nom de « nuisance & sympathetic tripping », et n'est pas non plus souhaité par les opérateurs. Pour (ii), la norme industrielle IEC60909-2016, qui est largement utilisée dans l'industrie lors de la conception et de l'évaluation des systèmes de protection des réseaux de distribution, est évaluée en utilisant les résultats des simulations RMS pour les schémas de production sélectionnés en (i). Ce rapport démontre tout d'abord les avantages des simulations RMS (par rapport aux résultats de la norme IEC60909-2016) pour les études de protection, en particulier lorsque les tensions du réseau s'écartent de manière significative de la tension nominale. Pour les simulations RMS, l'outil interne du FEN, FlexDYN*, est utilisé. Ensuite, les niveaux de défaut (c'est-à-dire les niveaux de courant de court-circuit, Ik") dans un réseau MT donné pour des états de fonctionnement du réseau sélectionnés avec des ressources d'énergie renouvelable élevées et faibles telles que le PV sont évalués. Ensuite, les impacts des différents niveaux de défaut dans les états d'exploitation du réseau sélectionnés sur la protection contre les surintensités des transformateurs MT-BT et des câbles MT ainsi que sur la protection de secours sont démontrés, et enfin une liste non exhaustive de mesures d'atténuation potentielles est fournie. Pour les simulations et les analyses, un réseau MT est utilisé, partagé par EKZ au format PowerFactory, comprenant des transformateurs MT-BT, tandis que les charges BT sont agrégées du côté BT des transformateurs. L'analyse montre qu'il est essentiel de prendre en compte la contribution du courant de court-circuit variable dans le temps (c'est-à-dire le niveau de défaut, Sk") provenant des réseaux supérieurs, prévue pour 2035+ lorsque le nombre de générateurs tournants sera plus faible dans la région ENTSO-E. Dans les cas extrêmes, par exemple lorsque Sk" est inférieur ou égal à 10% des valeurs actuelles, l'utilisation de la norme IEC60909-2016 pour évaluer les fonctionnalités des dispositifs de protection conduit à des résultats inexacts. En fonction de l'emplacement du bus BT (c'est-à-dire à proximité du transformateur HT-MT), des caractéristiques du transformateur MT-BT et de l'emplacement des PV (c'est-à-dire en MT ou en BT), la norme IEC60909-2016 peut sous-estimer ou surestimer de manière significative les niveaux de défaut au niveau du bus BT. Les phénomènes indésirables tels que la protection insuffisante et les déclenchements intempestifs et sympathiques pendant les courts-circuits dans les réseaux MT et BT sont détectés et mieux observés en utilisant des simulations RMS, en particulier lorsque Sk" des réseaux supérieurs est significativement plus faible. En raison de la contribution du courant de court-circuit des panneaux solaires photovoltaïques, on s'attend à ce que la coordination de la protection de secours pour la protection contre les surcharges des câbles soit gravement affectée. Les niveaux de courant de court-circuit du côté BT des transformateurs devraient être affectés. Si le service public utilise des HHS (Hochspannungs-Hochleistungs-Sicherung / fusible HT) en coordination avec les dispositifs de protection au niveau des départs BT, les paramètres de coordination doivent être réévalués pour différentes conditions d'exploitation (par exemple, une production PV élevée avec un Sk" faible).

# Contents

## List of abbreviations

| | |
|---|---|
| DER | Distributed energy resources |
| DG | Distributed generation |
| DSO | Distribution system operator |
| EMT | Analysis based on electromagnetic transient models or time-domain models |
| HHS | Hochspannungs-Hochleistungs-Sicherung, HV fuse for transformers |
| PV | Solar photovoltaic |
| RMS | Analysis based on root-mean-square or phasor (frequency-domain) models |
| SAIDI | System average interruption duration index |
| SCC | Short-circuit current |
| TSO | Transmission system operator |

# 1 Introduction

## 1.1 Background information and current situation

As part of the Energy Strategy 2050, Switzerland is planning to decommission large-scale nuclear power plants in the near future and increase the shares of variable renewable energy resources (VRE) in its electricity supply. Since a well-functioning protection system is an integral part of ensuring a secure operation and serves as an insurance for reliability, the impacts of such a paradigm shift on the current protection systems and practices, which were developed based on the behaviour of conventional rotating machines, have to be carefully investigated so that the main protection objectives are not compromised: timely detection and clearance of the faults, functional and efficient back-up protection coordination, avoiding problems such as protection under-reach (i.e., protection device is not activated during short-circuits due to low short-circuit current) and nuisance tripping (i.e., protection device is activated causing unnecessary interruption).

## 1.2 Purpose of the project

The overarching purpose of the project is to devise a qualitative and quantitative framework to analyze the potential impacts of converter-interfaced resources on the protection layouts of distribution grids (MV & LV), especially when the majority of large-scale conventional generation at high voltage (HV) and extra-high voltage (EHV) is de-activated during very high shares of distributed generation in MV and LV grids.

## 1.3 Objectives

The specific objectives of this project are as follows:

- to identify the sufficiently accurate modelling type and platform (e.g., RMS) for converter-interfaced sources (e.g., solar PVs) in protection studies, especially in comparison with the calculations of industry standard, IEC60909-2016,
- to study the impacts of reduction in short-circuit current contributions from EHV and HV grids to faults in MV and LV grids,
- to assess the fault levels (i.e., short-circuit current, SCC, levels) in a given grid for various operating states (e.g., very high share of distributed generation),
- to formulate the impacts of different fault levels in selected scenarios, and
- to elaborate on potential mitigation measures.

## 1.4 Structure of the report

In Section 2, the necessary terminology and background information are revisited based on the state-of-the-art calculations used by the industry, as well as the challenges for grid protection in presence of distributed generation, followed by the details of the studied grid, selected operational scenarios, and adopted converter models. In addition evolution of fault levels at EHV/HV grids in the future is elaborated upon, and the differences between the calculations based on the industry standard, IEC60909-2016 and the RMS/EMT simulations are discussed.

In Section 3 the comparative results of RMS simulations and the standard calculations are provided first, followed by the presentation of the results of RMS simulations for the selected operational scenarios on the studied MV grid. The results are analyzed in three groups: (i) fault levels at MV and LV nodes, (ii) maximum short circuit currents flowing through the MV-LV transformers, and (iii) maximum short circuit currents flowing though the cables and how they potentially impact the protection layout: the selected settings for the existing protection devices, and the back-up protection coordination.

Section 4 lists and elaborates upon the conclusions, followed by the suggested future work in Section 5.

# 2 Background, Methodology and Studied Grid

## 2.1 Background

The grid protection systems are integral part of the design of electricity grids at all voltage levels, and protect grid components against very high currents, very high voltages, very high or very low frequencies during unexpected events such as loss of generators or large demand, loss of transmission or distribution overhead lines or cables and transformers, etc. due to short-circuits, malfunctioning protection devices, etc. Short-circuits, which are the focus of this project, can occur at the substations, within transformer (e.g., HV-MV, MV-LV) windings, along the transmission and distribution overhead lines and cables, busbars due to various reasons such as unattended vegetation, animals, lightnings, deteriorated asset health, extreme weather events, cyber-physical attacks, etc.

The protection systems are designed for each voltage level and for each grid component (e.g., generators, transformers, overhead lines/cables) separately. Overcurrent (for transformers, lines), impedance (for lines/cables), differential (for transformers and generators), overfrequency (for generators), overvoltage (for generators) relays and/or fuses are a few of the most commonly used protection devices. In addition to the specific protection device selected for a given component, usually, a back-up protection is designed as well in case the protection device fails to detect the fault and activate the ”tripping” (i.e., to isolate the grid component from the grid by activating a circuit breaker). The protection layout includes the type of protection device selected for each grid component as well as the back-up protection system, which requires the coordination of the settings of each protection device. Therefore, each protection device usually has two or more tasks: (i) protecting a grid component, (ii) serving as a back-up to one or more protection devices that are responsible for protecting other grid components. Note that when designing protection layouts, the ”meshness” of the grids is also taken into account. That means, the protection layouts used for radial grids are different than the protection layouts used for meshed grids. Finally, it is important to note that, the practices in protection design exhibit large variations from country to country, and from utility to utility.

**Challenges in distribution protection in presence of distributed generation**: The proliferation of distributed generation (e.g. biogas, biomass, small CHP, small hydro etc.) in MV and LV grids already present challenges to the utilities, independent of the type of the generators, whether they are converter-based or not [1, 2, 3, 4, 5, 6]. The protection systems for MV and LV grids are designed mainly for a ”vertical operation”, when the only electricity supply to MV and LV grids are at the EHV/HV level. In presence of distributed generators at MV or LV grids, the short-circuits at MV or LV grids are not only fed by the generators in EHV/HV grids but also by those distributed generators connected at MV or LV grids. Three challenges are of interest within this context: (i) protection under-reach, (ii) nuisance & sympathetic tripping, and (iii) loss of coordination. **Protection under-reach** refers to a fault detection problem in presence of distributed generation in MV and LV grids, because the short-circuit current contributions by distributed generators (i.e., in-feed current) close to the short-circuit reduce the short-circuit current seen by the protection equipment (e.g., relays, fuses) located upstream of the distributed generators. This results in delayed or non-activation, especially if overcurrent protection relay or fuse is used. The same phenomenon results in larger impedance calculation by the relay, thus causing delayed or non-activation, as well, if distance protection relay is used, which is based on the impedance calculated by the voltage and the current measurements at the location of the relay. It is noted that a reduction in the short-circuit current contribution from upper grids will cause protection under-reach as well. **Nuisance & sympathetic trippings** occur when the protection device trips following an ”out-of-section” fault, that is a fault occurring not within the section that is protected by the protection device due to reverse current flow supplied by the distributed generator(s). In the context of distribution networks, if there are two feeders, for example feeder 1 and feeder 2, both accommodating distributed generators, the distributed generator(s) in feeder 2 will provide short-circuit current to a fault in feeder 1, which may result in activating the protection device protecting feeder 2. Even though there is no fault in feeder 2, this phenomenon leads to an undesired interruption of electricity to the customers connected to feeder 2. **Loss of coordination** refers to the phenomena, when the protection settings of multiple protection devices mainly for back-up protection are not valid due to changing conditions (e.g., topology, changing short-circuit currents seen by each protection device) in the system, because the settings are based on a set of assumed operating conditions.

Unprecedented levels of proliferation of converter-interfaced generation in both MV and LV grids further exacerbates these problems namely **protection under-reach**, **loss of coordination** and **nuisance &**

**sympathetic trippings**, especially, when the short-circuit current contribution from upper grids decrease seasonally or daily, simply due to the reduction in the number of online conventional generators. Impacts of fault current injections by solar PV converters on distribution protection, specifically on protection under-reach, loss of coordination, nuisance and sympathetic trippings are reported in detail in [7].

The necessary **terminology in grid protection, regarding the short-circuit currents** is provided below along with a brief explanation for how each quantity is utilized [8]. Figure 1 represents a typical short-circuit current provided by a synchronous generator for a fault far from the generator itself.

- *Initial three-phase symmetrical short-circuit current*,$I_k^{''}$, is the RMS value of the AC symmetrical component of a prospective (available) 3p short-circuit current.
  - Used to configure overcurrent protection equipment and dimension the operational equipment
- *Initial symmetrical short-circuit apparent power*, $S_k^{''}$, is the fictitious value determined as a product of the initial symmetrical short-circuit current, $I_k^{''}$, the nominal system voltage, V ( line-to-line in rms), and the factor,$\sqrt{3}$. $S_k^{''} = \sqrt{3} \cdot V \cdot I_k^{''}$ usually in MVA or GVA.
  - Used to configure overcurrent protection equipment along with $I_k^{''}$
- *Peak short-circuit current*, $i_p$, is the maximum possible instantaneous value of the prospective (available) short-circuit current. The $i_p$ at the node of interest for a three-phase (3p) fault, using the Thévenin equivalent at the node of interest, is given as $i_p = \kappa \cdot \sqrt{2} \cdot I_k^{''} = (1.02 + 0.95 \cdot e^{-3R/X}) \cdot \sqrt{2} \cdot I_k^{''}$ for non-meshed grids. The calculation of $i_p$ depends on the type of the grid (i.e., radial vs. meshed) as well as the characteristics of the grid (i.e., the $R/X$ ratios of the lines/cables), and $\kappa$ is multiplied by a factor of $1.15$ for meshed grids to take into account the inaccuracies caused by using the Thévenin equivalent from a network reduction with complex impedances[1]. [8].
  - Used in dynamic electrical and mechanical stress analysis of the components
- *Symmetrical short-circuit breaking current*, $I_b$, is the RMS value of an integral cycle of the symmetrical AC component of the prospective short-circuit current at the instant of contact separation of the first pole to open of a switching device.
  - Used to determine the current capacity of the switching devices

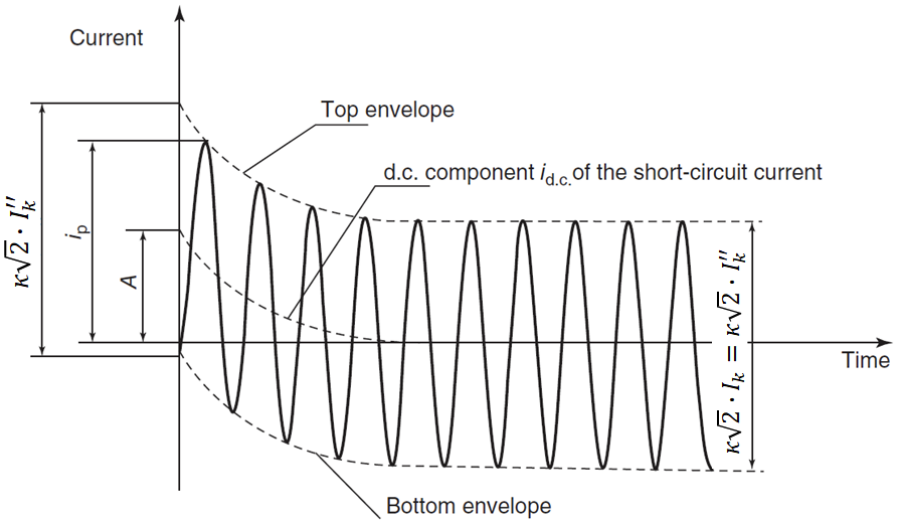


Figure 1: Representation of a short-circuit current by a synchronous generator for a fault far from the generator itself [8, 9]

Note that for all faults that occur far from synchronous generators, $I_b = I_k^{''}$. The main focus of interest within the context of this project is $I_k^{''}$, and consequently $S_k^{''}$. The methods to estimate the initial peak symmetrical short-circuit current, $I_k^{''}$ can be classified as follows:

[1] Network reduction and and Thévenin equivalents usually relay upon the calculation of bus admittance matric, $Y_{bus}$, which is then used to calculate the bus impedance matrix, $Z_{bus}$.

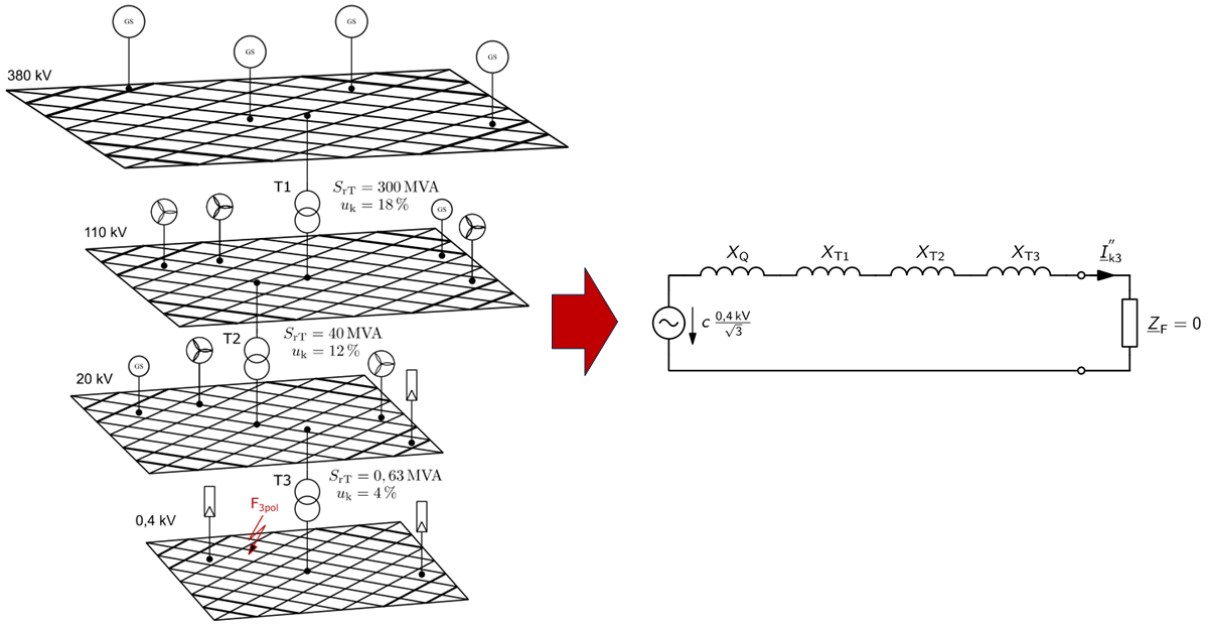


Figure 2: Equivalent representation of the one-line diagram for a $3\phi$ fault at LV grid [10] according to IEC60909 standard [8]

(i) **approximation methods**: outlined by IEC 60909, including the use of symmetrical component analysis for unbalanced faults,
(ii) **simulations**: using phasor-based models (i.e., RMS analysis) and using time-domain models (i.e., EMT analysis)

**The approximation methods in (i)** have been widely used by the grid operators in protection system design and it is state-of-the-art. These methods were devised based on the expected behaviour of synchronous generators, that are capable of providing 7-10 times the rated currents during short circuits, as demonstrated in Figure 1. Figure 2 illustrates the equivalent one-line diagram of the system during a $3\phi$ fault in the LV grid. $X_Q$ denotes the Thévenin equivalent reactance of the EHV grid at the point of connection to the HV grid to which the MV grid, which is feeding the LV grid where the fault is located, is connected. $X_{T1}$, $X_{T2}$, and $X_{T3}$ are the approximated Thévenin equivalent reactances of the network layers 2-6, simplified by using the reactances of the transformers at network layers 2, 4 and 6. $c$, denotes the voltage correction factor, according to the IEC60909 standard, varying between 0.95 and 1.00 for LV nodes, and 1.00 - 1.10 for MV nodes, and $Z_F$, stands for the fault impedance, $Z_F = 0$ when the short-circuit is "bolted". Total Thévenin impedance seen from the fault point, $Z_k = X_Q + X_{T1} + X_{T2} + X_{T3}$ and the maximum three-phase symmetrical short-circuit current, $I''_k = c \cdot \frac{V_n}{\sqrt{3} \cdot Z_k}$ according to the IEC60909 standard. The selection of $c$ is based on engineering practice and utility-dependent and maximum short-circuit currents for $1\phi$ faults are lower than the those for $3\phi$ faults and approximated by a coefficient based on IEC60909 standard and utility practices, when needed.

The industry standard IEC60900 is updated in 2016 [8] and the short-circuit current contributions by distributed generators are taken into account by means of superposition. The process requires the knowledge of either (i) the amount of short-circuit current that can be provided by each distributed generator in relation to its rated current, or (ii) the Thévenin impedance of each distributed generator, illustratively demonstrated and summarized in [11]. [12] and [13] are two examples of attempts to improve the IEC60909 calculations, based on steady-state models taking into account the contribution of short-circuit current from converters. [12] focuses on improving the network equivalents with converter-interfaced resource using voltage-dependent modeling, while [13] focuses on the steady-state modeling of short-circuits in unbalanced distribution systems, assuming that the converters can provide $1.1$ times their rated current. [10] demonstrates the impact of the solar PVs on short-circuit currents under various energy scenarios in Germany, using a slightly modified approach in the IEC60909 standard coupled with steady-state power flow simulations using representative CIGRE MV and LV grids.

Note that the magnitude of the short-circuit current that can be provided by converter is a commercial design parameter. The utility-scale and small-scale solar PV converters are designed to provide a short-

| Highest voltage for equipment, V [kV] | $I_k^{''}$ [kA] | $S_k^{''}$ [MVA] |
|---|---|---|
| 7.2 | 40 | 500 |
| 24 | 12 | 500 |
| 100 | 35 | 6'000 |
| 245 | 47 | 20'000 |
| 420 | 55 | 40'000 |

Table 1: Typical fault levels in EU [17]

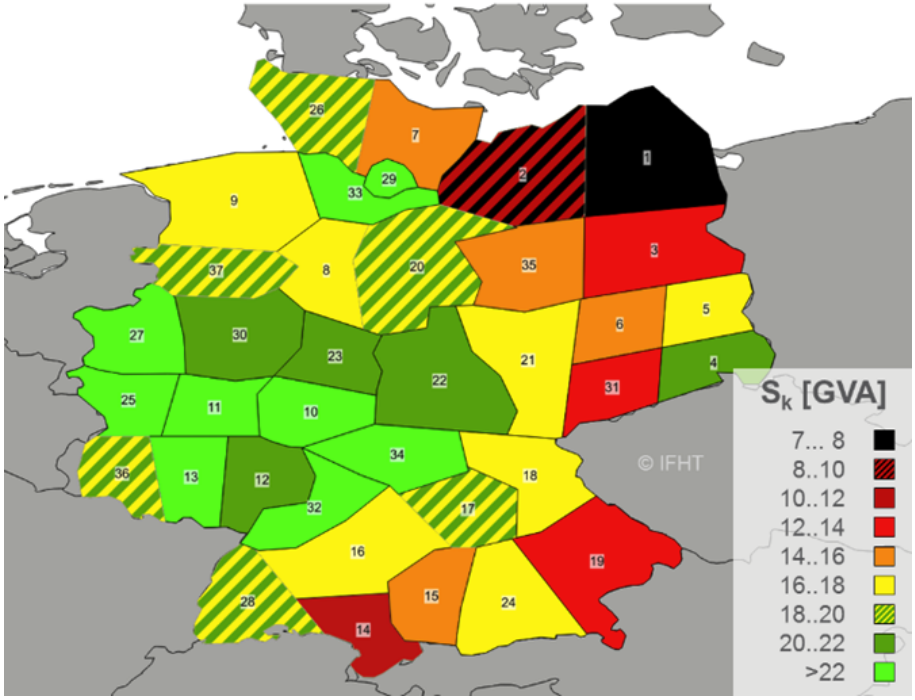


Figure 3: Average **fault levels** in Germany at EHV in 2019 (over 8760 h): 7 – 28 GVA [18]

circuit current which is usually $1.1 - 1.2$ times their rated current. It is important to emphasize that short-circuit current characteristics of the converters are not universal and the control system designs are proprietary [14]. Therefore, the level of short-circuit current contribution by converters, commercially available in different regions of the world, produced by different vendors exhibit different behaviour. As an example, [15] presents the laboratory test results of solar PV converters, produced by 6 different manufacturers and commercially available in Ontario, Canada, in 2012. The peak currents, $i_p$, are observed to be between $1.0 - 2.1$ times the rated current for a $3\phi$ fault.

The initial symmetrical short-circuit apparent power, $S_k^{''}$, calculated with the maximum short circuit current, $I_k^{''}$, that could flow through a given node in a grid when a three-phase (i.e., $3\phi$, a.k.a. symmetrical) short-circuit occurs at that node is referred to as "**fault level**" [16]. The fault level is used also as an indicator to assess the system strength at a fault location (e.g., at a substation) and depends on the voltage level. The higher the fault level is at a given fault location, the lower the Thévenin impedance and the stronger the power system is at that fault location. In general, the system fault levels has had relatively high values due to high fault level contribution from synchronous generators. The protection systems in all network layers (NE1-7) are designed accordingly, using the standards such as IEC60909 and IEC60076-5, given that the medium and low voltage grids are receiving short circuit currents from upper grid layers during short circuits in MV and LV grids, respectively. Table 1 provides some typical fault levels in the EU [17]. It is important to note that within each region the short-circuit current characteristics can demonstrate great variety. As a very good example, Figure 3 demonstrates the variation of fault levels in 37 regions in Germany in the year of 2019, calculated based on the market dispatch results [18].

**The second group of methods to calculate** $I_k^{''}$ rely upon time-domain or frequency-domain simula-

tions (i.e., EMT or RMS). Since the transient behaviour of the converters during short-circuits (i) are not universal, as explained above, (ii) may not be sinusoidal, and (iii) are dependent upon the nodal voltages, the approximation methods based on IEC60909 standard may not provide sufficiently accurate estimations. Therefore, the traditional approaches adopted by the industry as well as used in the majority of the commercial software packages may not accurately represent the behaviour of converters during faults [19]. Even though, RMS and EMT simulations may be computationally intensive and require higher level of digitization (e.g., sufficiently accurate models of the converters, RMS or EMT models of the grid components), the RMT or EMT simulations will be necessary to appropriately investigate the behaviour of converters during short-circuits so that the existing protection layouts can be properly assessed [15, 14]. Below are the summarizing points for the main challenges of the methods using IEC60909 standard and steady-state Thévenin equivalents for the converters:

- Difficulty of estimating the inverter impedance is a challenge for any fault analysis method relying on the calculations of Thévenin equivalents and $Z_{bus}$ [19]. Another important consequence for the assessment and design of a protection layout manifests itself in **faulted phase selection** process by the protection devices. The logic for faulted phase selection is responsible for identifying the fault type (e.g., phase A-to-ground, phase A-to-phase B-to-ground, etc.) and enabling the correct directional, distance and tripping protection elements, etc. Present faulted phase selection logic utilizes either voltage, current or a combination of voltage and current and is based on the assumption that a generator can be represented as a voltage source behind an impedance (i.e., Thévenin equivalence). The direct consequence of not being able to represent a solar PV converter as a voltage source behind an impedance, the existing faulted phase selection logics cannot be used to identify the faulted phase.
- Converters do not have universal short-circuit response characteristics. In addition to challenges due to reduced short-circuit current contribution by converter, to prevent to the power electronics from thermal overloads, the vendors opt to design the control systems such that the **negative sequence current** provided by the converters are fully or partially suppressed [14]. A consequence of this choice manifests itself in, for example, **directional protection**, which is based on the comparison of the negative sequence voltage with the negative sequence current to decide the direction of the fault current. However, not that the negative sequence current contribution by converter-interfaced resources is a controller design decision, and it is dependent on the inverter manufacturer if no specific grid code is present.
- RMS/EMT simulations take into account the real nodal voltages (pre-fault & during-fault) in the network rather than relying on assumptions based on nominal voltages (i.e., 1 p.u.) such as in methods based on IEC60909 standard. The functionality assessment of protection and protection coordination layouts can be healthily performed with more accurate representation of the actual phenomena, especially given that the converter behavior is highly dependent on the nodal voltages.

[20] presents the analysis of the impacts of one solar PV farm connected to a 24-kV substation in Florida on distribution grid protection functionalities, using EMT analysis, while [21] provides a comparative analysis of RMS and EMT models of converter-interfaced distributed generation, for testing the fault-ride-through (FRT) characteristics during a short-term voltage stability event. Two types of RMS models are compared for voltage source converters (VSC): (i) an average value model with full representation of the VSC inner control (AVM RMS), and (ii) simplified RMS model based on current sources (CS RMS). These two RMS models are then compared with a detailed EMT model with switching characteristics of the converter's switching devices. A small test grid (i.e., one MV feeder with an MV-LV transformer and one LV feeder connecting a VSC-interfaced distributed generation) is used for simulations. Figure 4 [21] shows that **the differences between the EMT and the two RMS simulations are not significant**, especially for capturing the initial short-circuit current peak. These conclusions are similar to the observation in the ACSICON project [22] when RMS models of FEN [23, 24, 25] implemented in the in-house steady- and dynamic state grid analysis tool, **FlexDYN**, and the EMT models of Hitachi Energy Research were benchmarked against each other [26]. Note that, the high-frequency (e.g., > 20kHz) converter EMT transients are usually filtered through the conventional current and voltage measurement devices and thus their impacts are not even be observable by the majority of the protection devices[2].

[2] Voltage measurement devices have a maximum of $6kHz$ cutoff frequency, while the current measurement devices may be in the range of 10-20 kHz

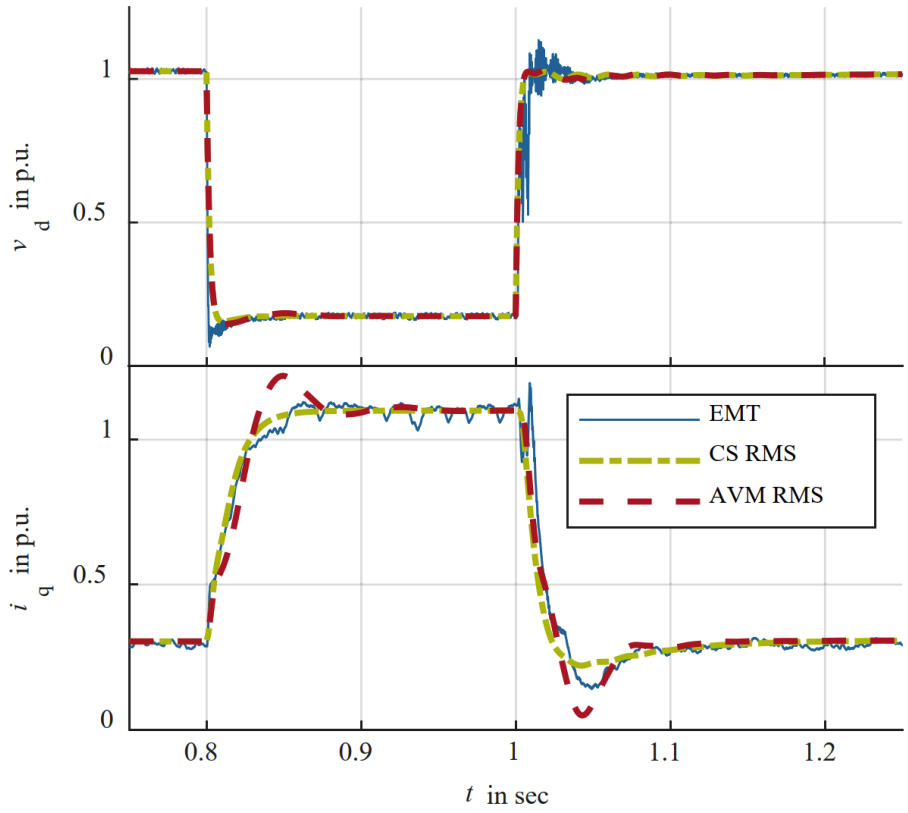


Figure 4: Comparison of converter voltage and current waveforms following a fault for RMS and EMT simulations [21]

**Reduction in SCC capacity from upper grids**: It is already reported in the literature that the short-circuit current capacities in transmission networks (EHV) [27, 28, 29, 30, 31] and in sub-transmission and distribution networks [32, 33] are changing and expected to further evolve due to the implementation of new energy policies relying mainly on converter-interfaced generation technologies. The common conclusion in all these studies is that the proliferation of converter-interfaced generation will introduce time-variant short circuit current capacities varying significantly according to the available generation types in the system. This phenomenon is unprecedented in the history of transmission and distribution grids, it is expected to exacerbate when the number of spinning generators will be lower in the whole European interconnection (daily or seasonally) and shall be taken into consideration to avoid jeopardizing the protection layouts in place.

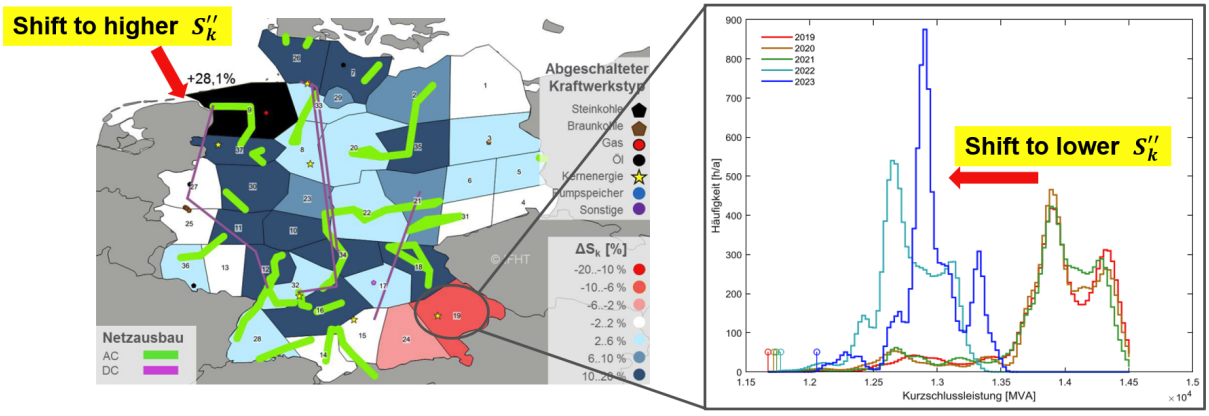


Figure 5: **Left**: Evolution of fault levels in Germany at EHV: 2019 – 2023. **Right**: Evolution of statistical distribution of fault levels at EHV in **Region 19 - Southwest**: 2019 – 2023 [18].

Figure 5 and Figure 6 illustrate the already occuring phenomena in Germany and in the UK. Note that in both regions, depending on the topology of the grid (e.g., new HVDC connection to transport the large

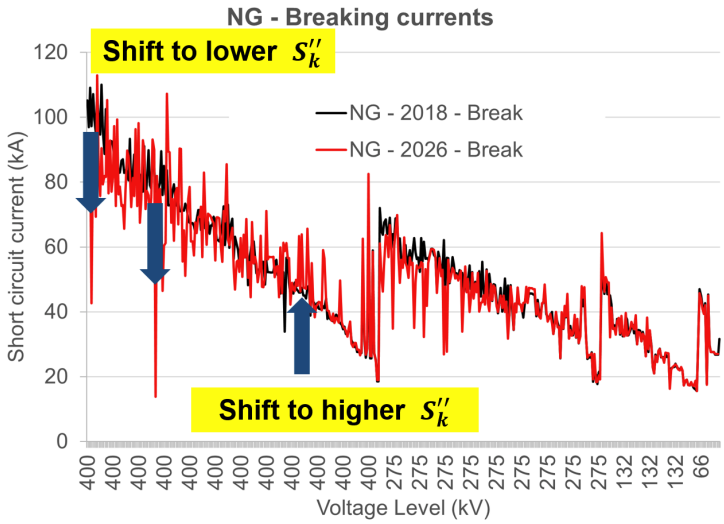


Figure 6: Evolution of fault levels in the service territory of National Grid in the UK at EHV, HV and MV [31].

amount of wind generation to the mainland Germany) as well as the location of the connection of the converter-interfaced generation (i.e., wind farms in UK, wind farms in the North Sea in Germany, solar PVs in southern Germany), increase and decrease in short-circuit capacities are observed. In summary, the evolution of the fault levels in EHV/HV grids are due to the following:

- Decommissioning (permanent loss) of synchronous generators
- Daily or seasonal operation of synchronous generators
  - spinning at lower production [can still provide full short circuit power during a fault]
  - offline [no short circuit current contribution] due to PV or wind production
- Grid topology changes (e.g., construction of HVDC links, new overhead lines), significantly affecting the Thévenin equivalents of the networks
- The level of converter-interfaced generation (e.g., high production during low demand)

A **grid-following current-controlled converter model** is used, based on [34] and further developed and tuned in [22, 26] for the in-house RMS tool FlexDYN, as illustrated in Figure 7. **VSM-MEASURE** stands for the module responsible for the rotation from grid dq-frame to local dq-frame, while **MAIN** represents the physical model of the converter circuit in the grid dq-frame, **VSM-DCSIDE** represents the capacitor assuming constant power received from the DC-side, and **VSM-IREFCTRL** represents the saturated PI controller, controlling the DC voltage by adjusting the active power fed into the grid. The short-circuit current contribution by solar PV converters are limited at $1.1$ times the nominal current. However the impact of higher short-circuit contribution (i.e., $2.5$ times the nominal current) is also tested, which can potentially represent the (i) grid-forming converters that are voltage source converters (VSC) [19], and (ii) induction machine-driven wind parks.

## 2.2 Methodology

Figure 8 demonstrates the overall methodology and the steps for analyses. The cantonal distribution system operator, EKZ, provides an MV grid with MV-LV transformers with a loading snapshot at each LV node, and the protection layout in PowerFactory[3]. As a first step, the grid model in PowerFactory format is converted to the json format used by the in-house steady-state and dynamic analysis tool, FlexDYN, and treated as the base-case grid model. The converter models developed in [22] are tuned and used. For each operational scenario with selected DG generation level and type, and available short-circuit current capacity from EHV/HV grids corresponding modifications of the base-case grid model are made.

[3]https://www.digsilent.de/en/powerfactory.html

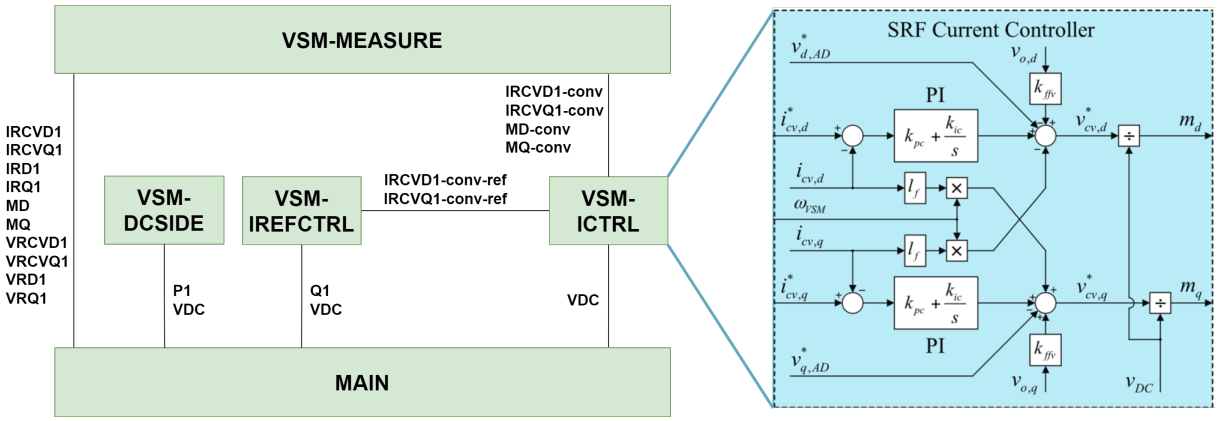


Figure 7: Converter model: grid following, current-controlled source - **Left**: Implementation in **FlexDYN** [22]. **Right**: The "VSM-ICTRL" (current controller) implementation [34]

RMS simulations for each modified grid are performed for a $3\phi$ fault at each MV and LV node at a time and the maximum short-circuit currents, $I_k^{''}$, for each component as well as the fault currents are extracted. Once we simulate each fault for one cycle (i.e., 20 ms), we observed the evolution of the short-circuit current by using two methods: (i) extracting the initial current peak, and (ii) extracting the maximum value of the current during the one cycle following the fault. Finally, the functionalities of the protection layout are assessed based on these results.

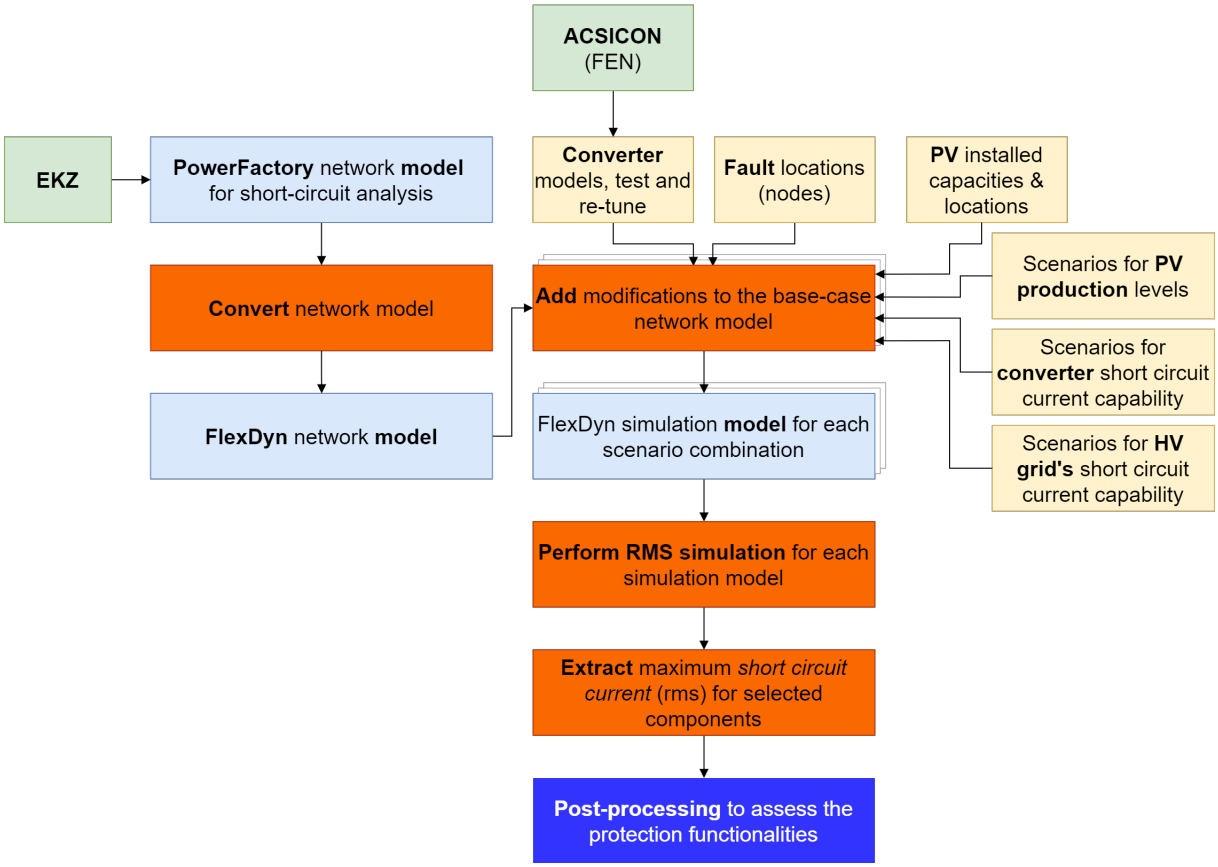


Figure 8: The overall methodology and the steps for analyses

## 2.3 The studied grid and the selected scenarios

The analyses are performed using an MV grid provided by the cantonal distribution system operator, EKZ. The provided grid has 25 MV nodes and 25 MV cables (11.2 km of cabling) at 16 kV, with 28

MV-LV transformers, and 28 LV nodes at 0.4 kV (Figure 9). The load in each LV grid is aggregated at the LV bus of each MV-LV transformer. The snapshot of the provided grid has a total power demand of $9.8MW$ and $2.0MVAr$. The protection layout is also provided, consisting of an overcurrent protection device for each cable and an HHS (i.e., Hochspannungs-Hochleistungs-Sicherung) device connected at the MV side of each MV-LV transformer. Due to space considerations and efficacy of illustration of results a few cables and transformers are selected: The cable segments 795, 810, 800 and 805, and the transformers 1522 and 1524 are denoted in **Feeder 2** while the cable segments 773 and 787, and the transformers 1526 are denoted in **Feeder 1**. The in-house steady-state and dynamic analysis tool, FlexDYN, is used for RMS simulations.

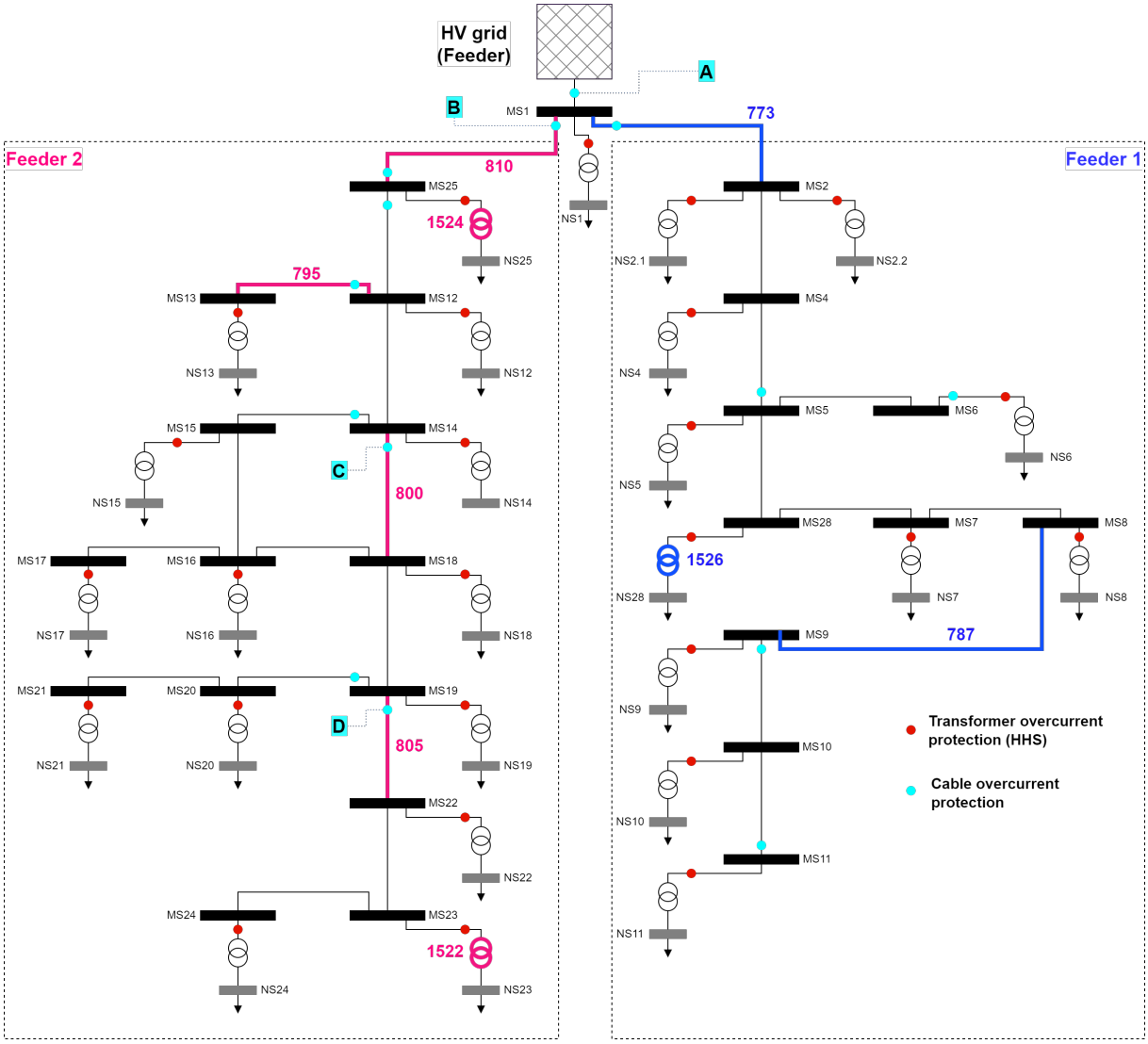


Figure 9: The studied MV grid provided by EKZ, with selected protection devices and marked cable segments and MV-LV transformers for further demonstration of the results

An example for the back-up coordination for a selected set of protection devices is provided with overcurrent information with breaking time as demonstrated in Figure 10. Four protection devices are picked for demonstration: **A** is the overcurrent device at the HV feeder, and it is set such that it will activate after **1 s** once the short-circuit current, $I_k''$, flowing through the cable is **1'000 A**, while the **B**, **C** and **D** will activate much quicker (in less than 0.4 s) if the short-circuit current at the same level, while **D** is the fastest acting, **C** is slightly delayed, acting as a protection backup to **D**, and **B** is acting as a protection back-up to **C**. For a short-circuit current of 450 A, **D** is set to activate at 0.4 s, backed up by **C** at 0.6 s, which is backed up by **D** at 0.8 s. Note that the described back-up layout is designed under the assumption that the same short-circuit current flows throughout the cable segments in series and the only source of supply for the short-circuit current is the HV-MV substation connected to the MV node 1 in Figure 9.

Table 2 provide the list of operation and/or proliferation scenarios selected to be investigated. Five

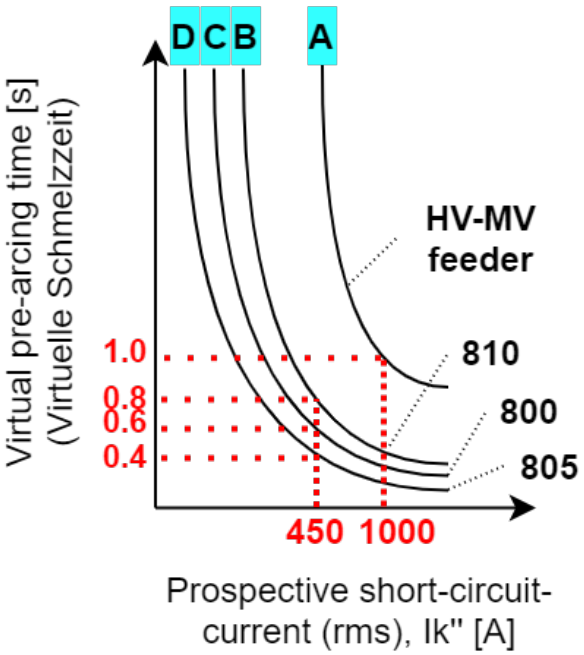


Figure 10: An illustration of the protection and back-up protection coordination layout with MV cable overcurrent protection devices in the studied MV grid in Figure 9. Note that the characteristics of all devices are known. Due to space limitation and efficiency only those of A, B, C and D are shown.

parameters are selected to create the scenario cases (SC):

1. The ratio of the instantaneous power generated by the distributed generation (e.g., PV, wind) to the demand:
   - Low proliferation of distributed generation: $P_{Demand} \gg P_{Dist.generation}$
   - High proliferation of distributed generation - **at night**: $P_{Demand} \gg P_{Dist.generation}$
   - High proliferation of distributed generation [high excess of local generation not consumed locally] - **during a summer day**: $P_{Demand} \ll P_{Dist.generation}$
2. The location of the distributed generation (voltage level):
   - The distributed generators are mainly connected at the LV nodes. As noted above, the LV grids are not provided and the loads in each LV grid is aggregated at the LV bus of each MV-LV transformer. Same is valid for PVs. Therefore, the impact of the impedances of the LV cables on the short-circuit current contribution of the PVs located in the LV grids are not captured.
   - The distributed generators are mainly connected at the MV nodes. Note that the step-up transformer is ignored, and the PVs are modeled as directly injecting the power to the MV grid. Therefore, the impact of the step-up transformers (e.g., short-circuit characteristics) on the short-circuit current contribution of the PVs are not captured.
   - The distributed generators are connected to both MV and LV nodes.
3. The location of the distributed generation (MV feeder):
   - The distributed generators are connected to the MV or LV nodes along Feeder 1.
   - The distributed generators are connected to the MV or LV nodes along Feeder 2.
4. The available short-circuit current capacity, $S''_{k-max}$ available in upper grids (EHV/HV): 100% corresponds to today's level, while 10% denotes that only 10% of today's capacity is available.
5. The short-circuit current capability of the converters: A PV converter is assumed to be able to supply a short-circuit current 10% higher than its rated current, while induction motor-driven wind parks or new converter technologies are assumed to be able to supply short-circuit currents as much as 2.5 times their rated currents.

High proliferation of distributed generation scenarios in Table 2 correspond to total MWp installed capacity (or maximum generation) of distributed generation at MV and/or LV nodes of interest that is 2-3 times the base-case demand at corresponding MV and/or LV node, resulting in high amount of excess generation.

The selected parameterization allows to investigate the evolution of short-circuit currents under different scenario combinations and their consequent impacts on the functionalities and the efficacy of the protection layouts. For each scenario (SC#) and $S_k^{''}$ variation an RMS simulation is performed for a $3\phi$ fault at each MV and LV node at a time, corresponding to a total of 50 faults, resulting in $(8 \times 3 + 4)\ S_k^{''}\ variations \cdot 50\ faults = 1'400$ RMS simulations performed with variable integration step in FlexDYN.

Table 2: Selected operational scenarios and layouts for the MV grid based on (i) the location of the distributed generation (the MV feeder and connected to the MV or LV nodes), and (ii) variations of available SCC capacity from EHV/HV grids, $S_{k-max}^{''}$. The installed distributed generator capacity in kWp in SC10 ad SC11 are same as those in SC5 and SC6, respectively. Short-circuit current contribution by DG, $SCC_{DG}$ is provided with respect to the nominal current of the DG converter. $P_D$ denotes the active power demand,$P_{PV\ Gen}$ and $P_{Wind\ Gen.}$ stands for the active power generation by PV and Wind, respectively.

| Scenario ID | Operation scenario | $SCC_{DG}$ | DG at LV or MV | MV Feeder | $S_{k-max}^{''}$ variations |
|---|---|---|---|---|---|
| **SC0** | Base case | N/A | None | N/A | 100% |
| **SC1** | $P_D \gg P_{PV\ Gen.}$ | 1.1 | LV | 1 & 2 | 100% |
| **SC2** | $P_{PV\ Gen.} \gg P_D$ | 1.1 | LV | 1 & 2 | 100%, 10%, 1% |
| **SC3** | $P_{PV\ Gen.} \gg P_D$ | 1.1 | LV | 1 | 100%, 10%, 1% |
| **SC4** | $P_{PV\ Gen.} \gg P_D$ | 1.1 | LV | 2 | 100%, 10%, 1% |
| **SC5** | $P_D \gg P_{PV\ Gen.}$ | 1.1 | MV | 1 & 2 | 100% |
| **SC6** | $P_{PV\ Gen.} \gg P_D$ | 1.1 | MV | 1 & 2 | 100%, 10%, 1% |
| **SC7** | $P_{PV\ Gen.} \gg P_D$ | 1.1 | MV | 1 | 100%, 10%, 1% |
| **SC8** | $P_{PV\ Gen.} \gg P_D$ | 1.1 | MV | 2 | 100%, 10%, 1% |
| **SC9** | $P_{PV\ Gen.} \gg P_D$ | 1.1 | MV & LV | 1 & 2 | 100%, 10%, 1% |
| **SC10** | $P_D \gg P_{Wind\ Gen.}$ | 2.5 | MV | 1 & 2 | 100% |
| **SC11** | $P_{Wind\ Gen.} \gg P_D$ | 2.5 | MV | 1 & 2 | 100%, 10%, 1% |

Note that the system can experience any of the following combinations in different seasons or in a given day:

- SC1 and SC2
- SC1,SC2 and SC3
- SC1,SC2 and SC4
- SC5 and SC6
- SC5,SC6 and SC7
- SC5,SC6 and SC8
- SC10 and SC11

# 3 Analysis and results

In the following subsections, first the comparison between the results of the RMS simulations and those of the IEC60909-2016 are provided. The RMS simulations are performed by FlexDYN, while the IEC60909-2016 results are obtained by using PowerFactory. Following, a summary of the short-circuit currents, as the results of the RMS simulations, for selected MV and LV nodes are provided to demonstrate the evolution of the short-circuit currents for all scenario combinations provided in Table 2. Finally, the evolution of the maximum short-circuit currents flowing through selected transformers and cables are shown to illustrate the challenges for the present protection layouts.

## 3.1 Calculation of fault levels: RMS vs. IEC60909-2016

Base-case scenario, SC0, SC2 and SC6 in Table 2 are selected for comparison of the results, first for selected MV and LV nodes, followed by the results for all nodes. Figure 11 shows the results of the RMS simulations compared with those of IEC60909-20156 calculations. A $3\phi$ fault is simulated at the MV node MS9 for each selected scenario and the fault currents ($I_k^{''}$) are presented. Note that, the results for today's conditions with full availability of short-circuit current contribution from upper grids, $S_k^{''} = 100\%$ is denoted by green. There are no significant differences between the results of the RMS simulations and IEC standard calculations, when the short-circuit current contribution from upper grids, $S_k^{''}$ is at today's level (100%). It can be observed that the IEC60909 calculations overestimate the contributions from converters except for the base-case (SC0) since the method assumes nominal voltage at the time of the fault. As $S_k^{''}$ decreases to $10\%$ of today's value (implying that the short-circuit contribution of EHV decreases due to fewer number of online rotating machines), the differences between RMS and IEC6090 results are significant. The fault levels decrease such that the present overcurrent protection devices may not detect the faults within the present time settings. This phenomena is observable only with the RMS simulations.

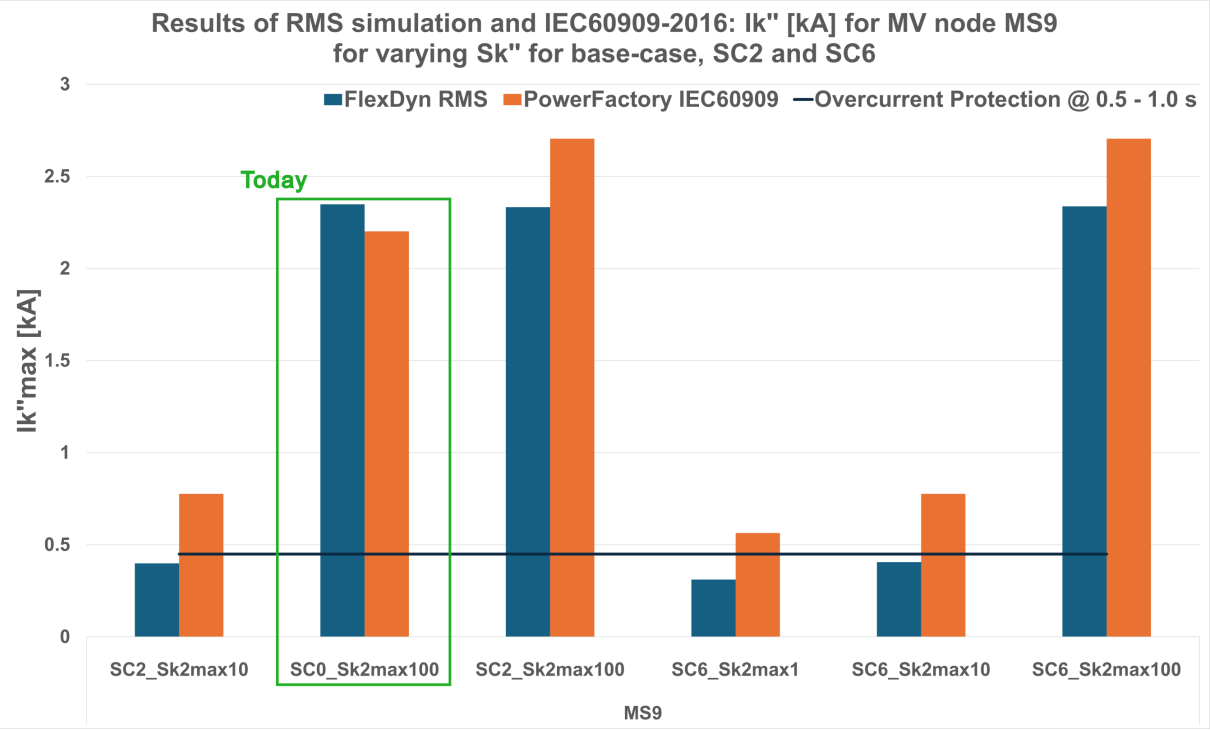


Figure 11: Comparison of the results of RMS simulations and IEC60909-2016: $I_k^{''}$ [kA] for the MV node MS9, for a $3\phi$ fault, for varying $S_{k-max}^{''}$ and for scenarios SC0 (base-case), SC2 and SC6.

Figure 12 presents the results for three LV nodes. A $3\phi$ fault is simulated at each LV node at a time, for each scenario combination. Note that, the results for today's conditions with full availability of short-circuit current contribution from upper grids, $S_k^{''} = 100\%$ is denoted by green. It is observable that the results are not similar for each LV node. For LV nodes NS24 and NS25, the results of the RMS

simulations and the IEC standard calculations show significant discrepancy, especially for the scenario SC6 with $S_k^{''} = 1\%$ and $10\%$, while for NS28, this discrepancy is prominent only for the scenario SC6 with $S_k^{''} = 1\%$. As described in Table 2, in SC6 the PVs are mainly connected at the MV nodes, and contributing to the faults at the LV side of the MV-LV transformers. Therefore, the transformer short-circuit characteristics play an important role, resulting in different responses to the short-circuits, under varying conditions. Note that, modeling the LV grids may further exacerbate the differences, since the PVs are modeled as aggregated at the LV side of the MV-LV transformers and the impact of the LV cables are not captured. It is important to emphasize that the fault levels are underestimated by IEC60909 when $S_k^{''}$ is reduced, mainly due to nominal voltage assumption, while the operational nodal voltage is higher than 1.0 p.u. due to high excess PV.

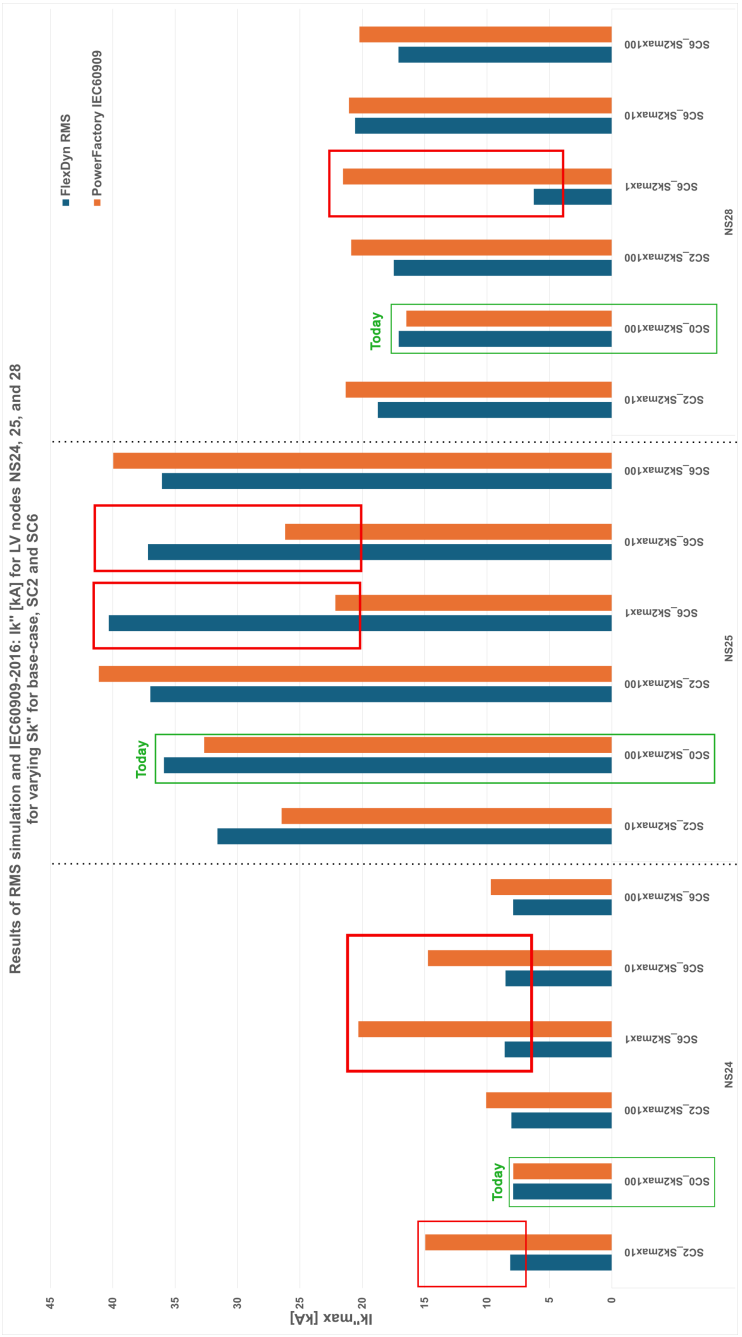


Figure 12: Comparison of the results of RMS simulations and IEC60909-2016: $I_k^{''}$ [kA] for the LV nodes NS24, NS25 and NS28, for varying $S_{k-max}^{''}$ and for scenarios SC0 (base-case), SC2 and SC6

Figure 13 and 14 illustrate the results individually for the LV nodes NS5 and NS7. Note that in Figure 13, the fault level is overestimated by IEC60909 in SC6 where the PV is located at the MV side, while in Figure14, the fault level is underestimated by IEC60909 in SC2, where the PV is located at the LV side of

the MV-LV transformer. Similar to the case for the MV nodes, there is no significant difference between the results when $S_k^{''}$ is at today's level $(100\%)$. However, significant differences between the RMS results and the standard calculations are observed when $S_k^{''}$ drops. Depending on the location of the LV bus (e.g., proximity to HV-MV substation), the MV-LV transformer's characteristics, and where the PVs are located (i.e., at MV vs. LV), IEC60909 may significantly underestimate or overestimate the fault level. This phenomenon is especially important for the protection coordination between the LV cable protection devices and the transformer protection devices. For completeness, Figure 16 and 15 demonstrate the results for all LV and MV nodes, respectively. Note that, the pattern of differences between the RMS simulations and the IEC standard calculations of short-circuit currents do not vary among the MV nodes, while the patterns for differences for LV nodes can be significantly different.

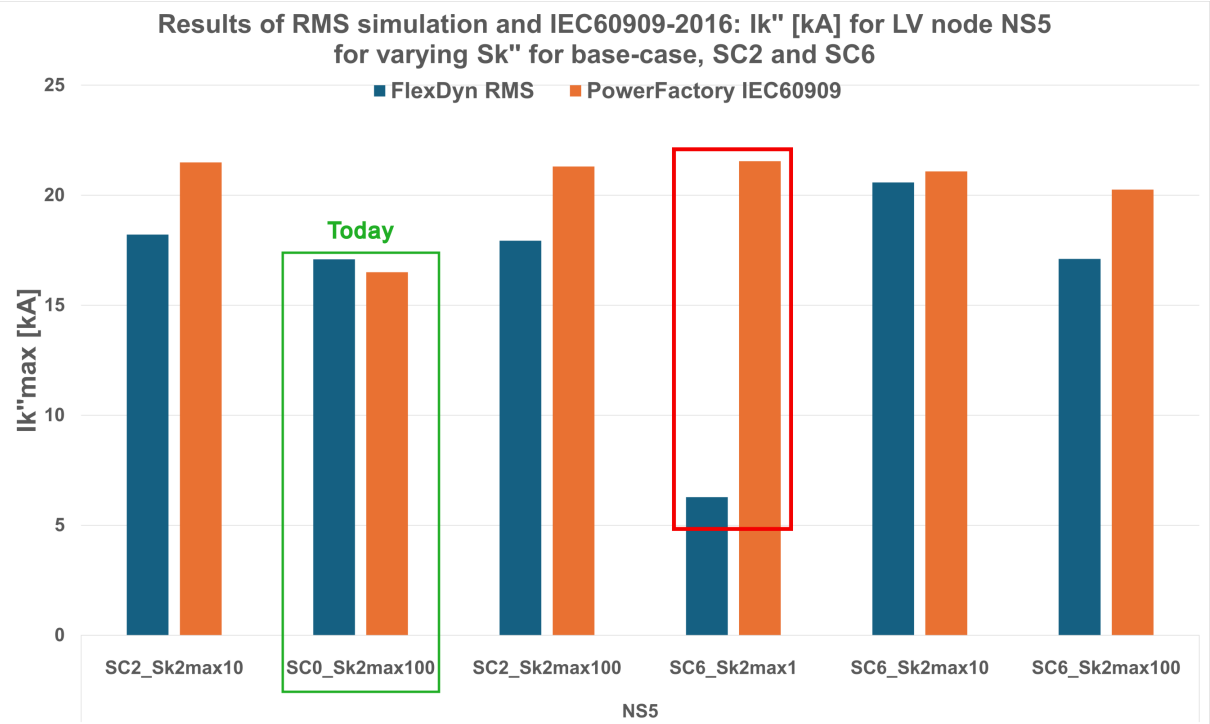


Figure 13: Comparison of the results of RMS simulations and IEC60909-2016: $I_k^{''}$ [kA] for the LV node NS5, for varying $S_{k-max}^{''}$ and for scenarios SC0 (base-case), SC2 and SC6

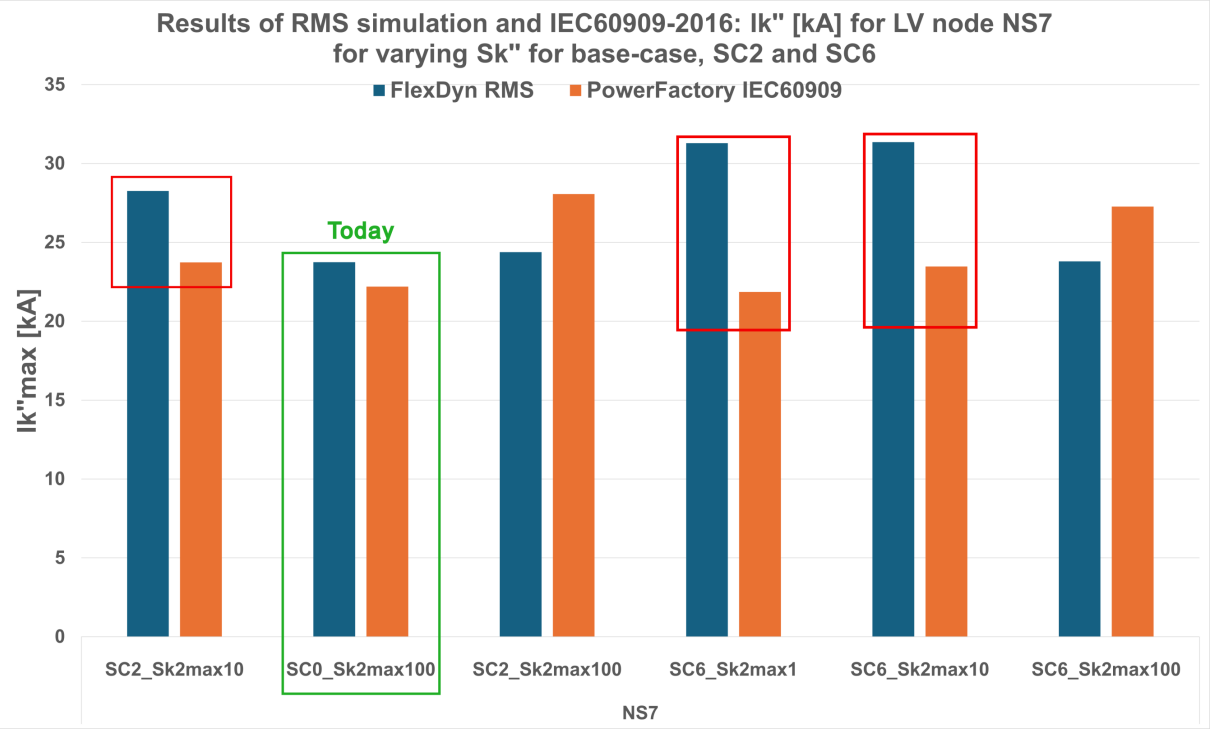


Figure 14: Comparison of the results of RMS simulations and IEC60909-2016: $I_k^{''}$ [kA] for the LV node NS7, for varying $S_{k-max}^{''}$ and for scenarios SC0 (base-case), SC2 and SC6

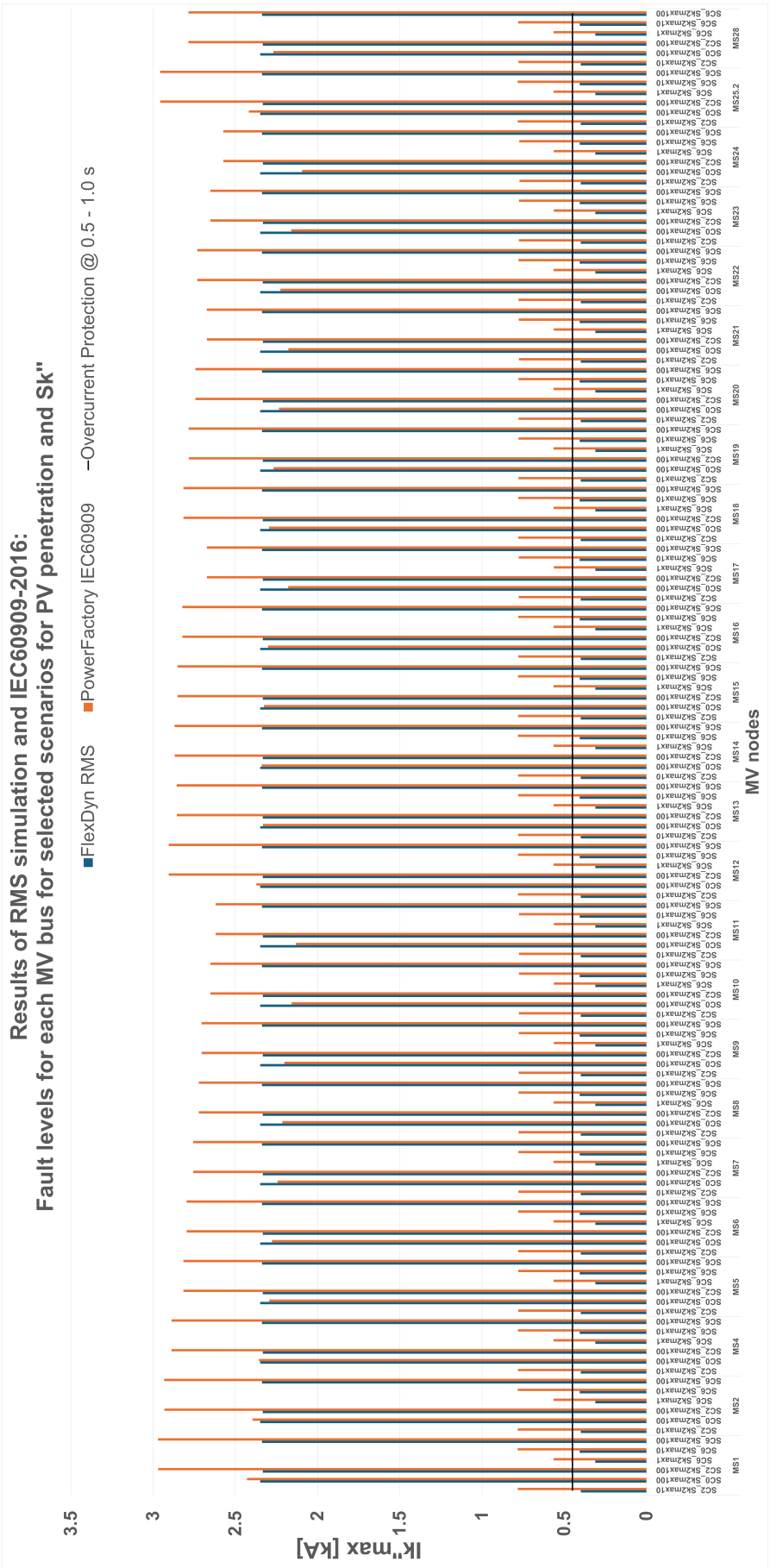


Figure 15: Comparison of the results of RMS simulations and IEC60909-2016: $I_k^{''}$ [kA] for all MV nodes, for varying $S_{k-max}^{''}$ and for scenarios SC0 (base-case), SC2 and SC6

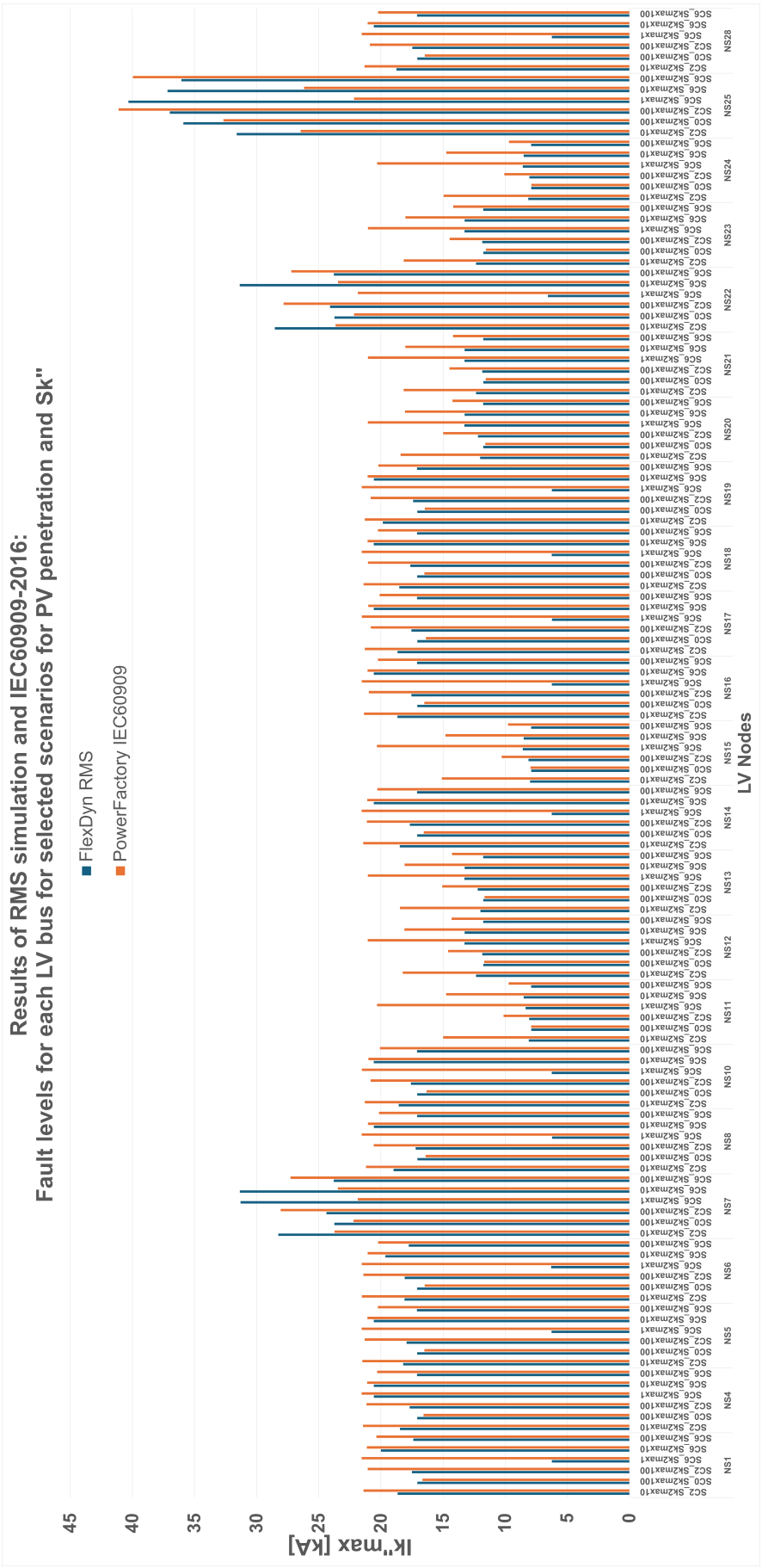


Figure 16: Comparison of the results of RMS simulations and IEC60909-2016: $I_k^{''}$ [kA] for all LV nodes, for varying $S_{k-max}^{''}$ and for scenarios SC0 (base-case), SC2 and SC6

## 3.2 RMS results: Fault levels at MV and LV nodes

In the previous section, it is demonstrated that the short-circuit calculations by RMS simulations capture the short-circuit contribution of the converters and the overall grid phenomena more accurately, especially when the short-circuit current contribution from upper grids decrease significantly. In this section, the RMS results for selected MV and LV nodes will be demonstrated based on their proximity to the HV-MV substation and for all scenarios in Table 2.

Figure 17, 18 and 19, demonstrate the results of a $3\phi$ fault at MV nodes MS25, MS16 and MS24 at a time for each scenario and for each $S_k^{''}$ combination given in Table 2. MS25 is located in close proximity of the HV-MV transformer, while MS16 is located in the middle of the Feeder 2 and MS24 is located at the very end of Feeder 2. The results are provided in relation to the today's conditions, captured by the base-case scenario, SC0 and $S_k^{''} = 100\%$, corresponding to $1.0$. It is observable that the patterns of short-circuit current evolution are similar in MV nodes, due to the fact that the studied grid in Figure 9 does not span a large area and it is not elongated, which are the two circuit characteristics that affect the simulation results. However, significant differences in the patterns of short-circuit current evolution for various scenarios are observed in Figures 20, 21 and 22, for the LV sides of each MV node above.

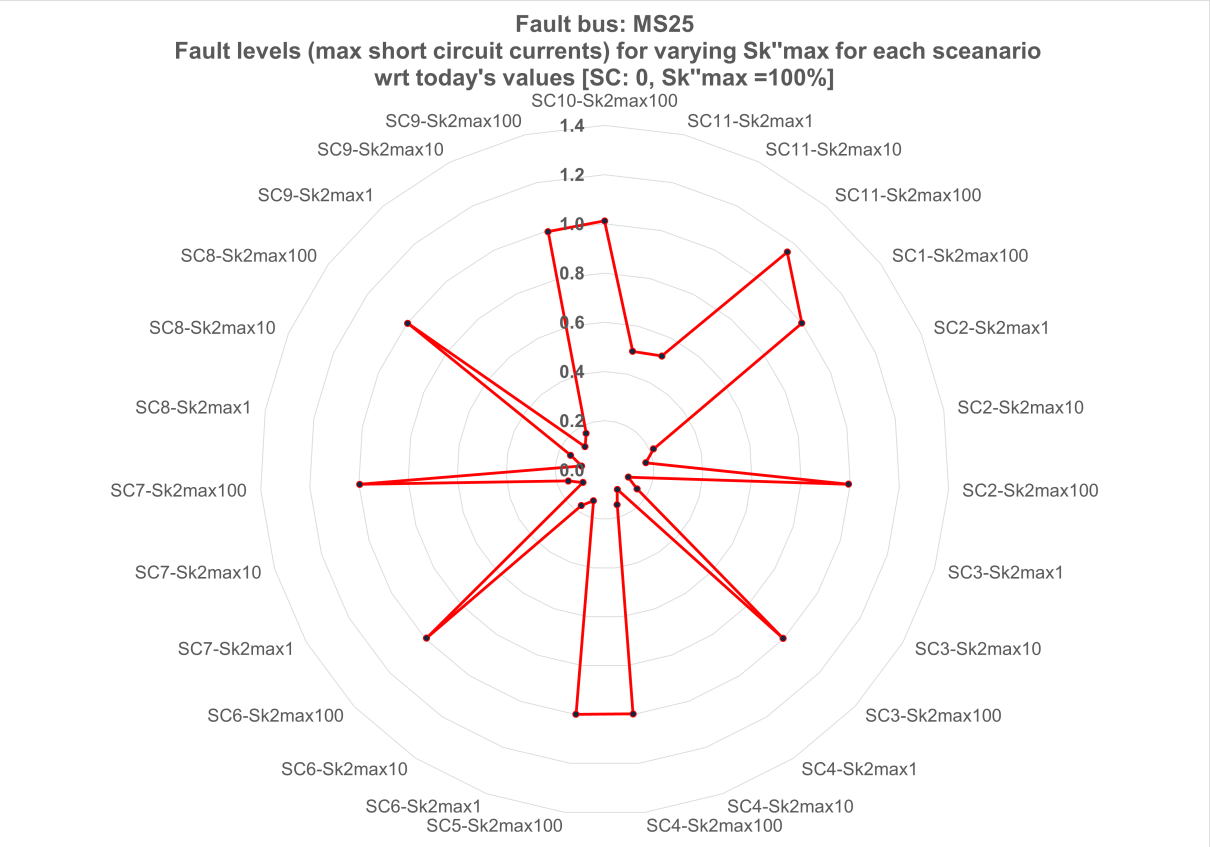


Figure 17: Maximum short-circuit currents, $I_k^{''}$ for the MV node MS25 [**close to the HV-MV transformer**] for all combinations of $S_{k-max}^{''}$ for each scenario (SC1-SC11) with respect to the today's value (1.0) for the base-case scenario, SC0 and $S_{k-max}^{''} = 100\%$

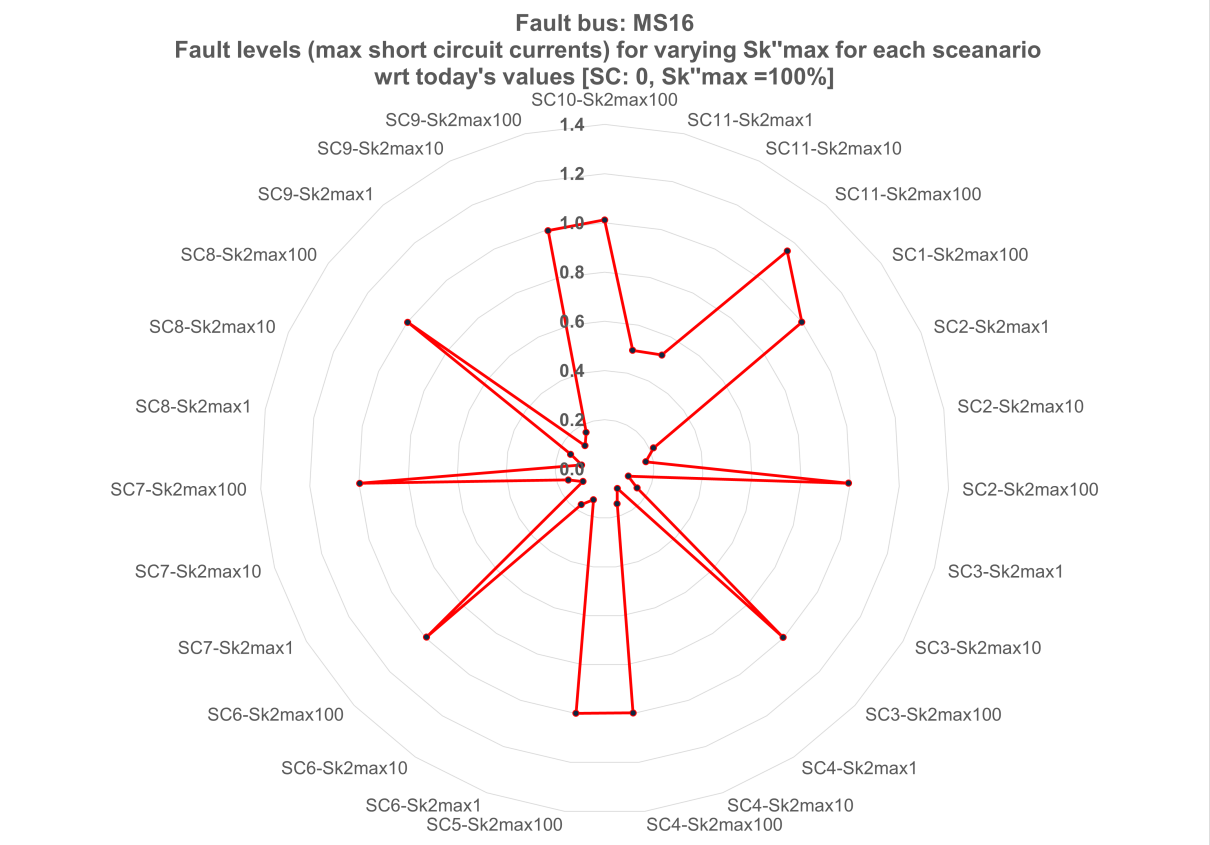


Figure 18: Maximum short-circuit currents, $I_k^{''}$ for the MV node MS16 [**in the middle of the Feeder 2**] for all combinations of $S_{k-max}^{''}$ for each scenario (SC1-SC11) with respect to the today's value (1.0) for the base-case scenario, SC0 and $S_{k-max}^{''} = 100\%$

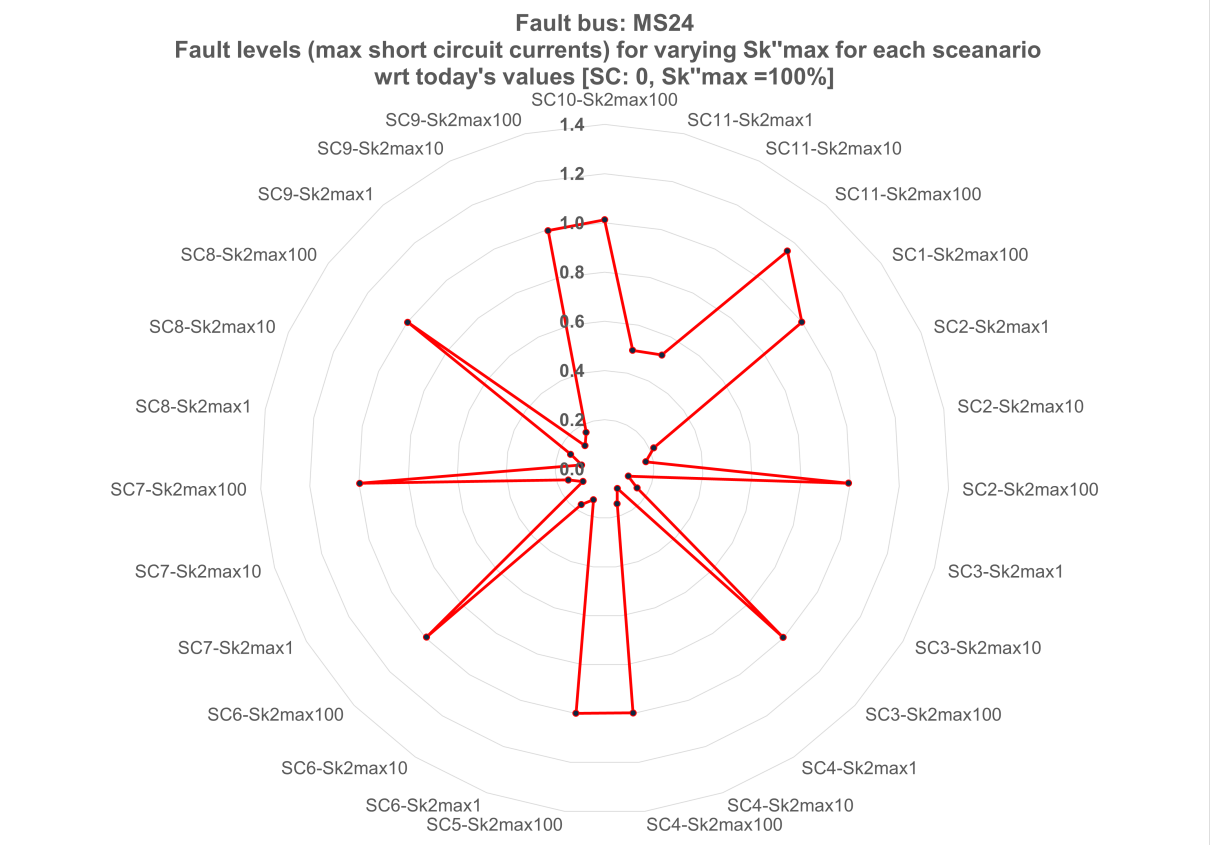


Figure 19: Maximum short-circuit currents, $I_k^{''}$ for the MV node MS24 [**at the very end of Feeder 2**] for all combinations of $S_{k-max}^{''}$ for each scenario (SC1-SC11) with respect to the today's value (1.0) for the base-case scenario, SC0 and $S_{k-max}^{''} = 100\%$

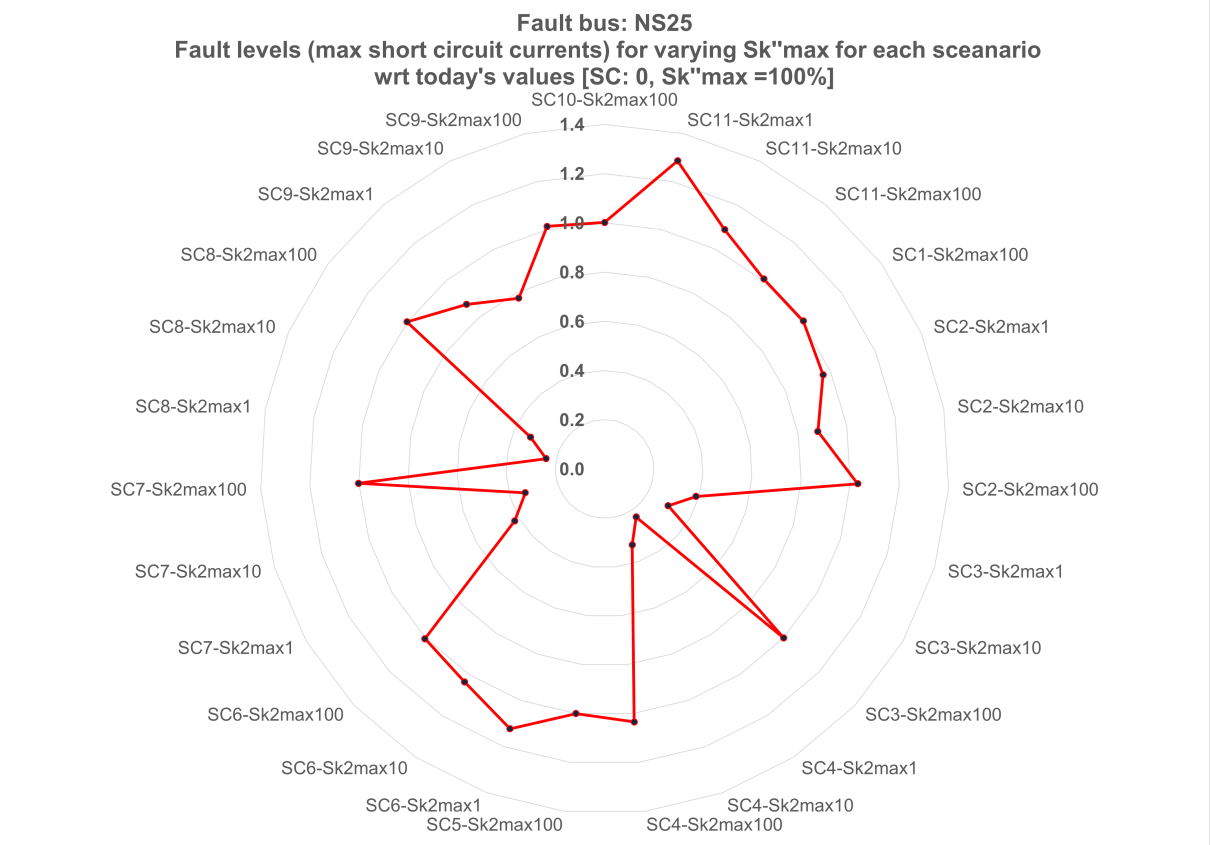


Figure 20: Maximum short-circuit currents, $I_k^{''}$ for the LV node NS25 [**close to the HV-MV transformer**] for all combinations of $S_{k-max}^{''}$ for each scenario (SC1-SC11) with respect to the today's value (1.0) for the base-case scenario, SC0 and $S_{k-max}^{''} = 100\%$

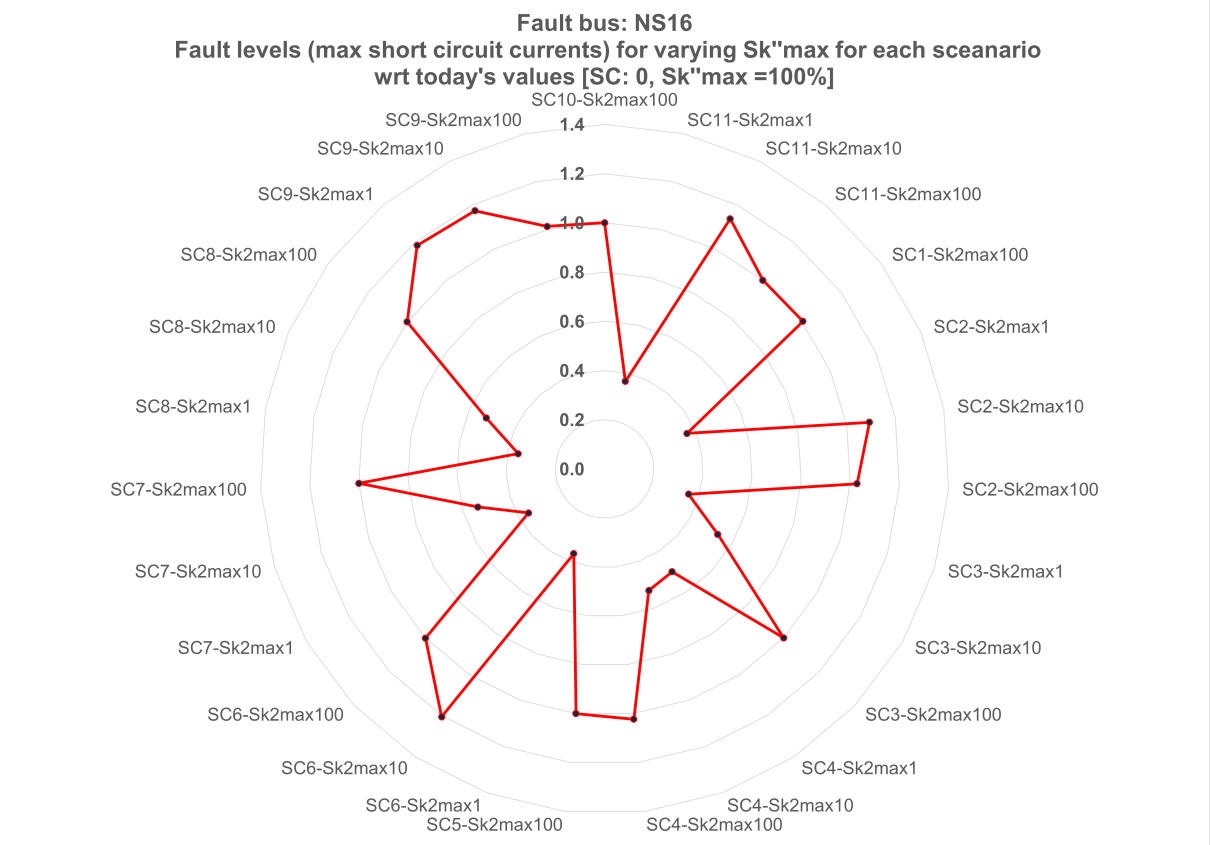


Figure 21: Maximum short-circuit currents, $I_k^{''}$ for the LV node NS16 [**in the middle of the Feeder 2**] for all combinations of $S_{k-max}^{''}$ for each scenario (SC1-SC11) with respect to the today's value (1.0) for the base-case scenario, SC0 and $S_{k-max}^{''} = 100\%$

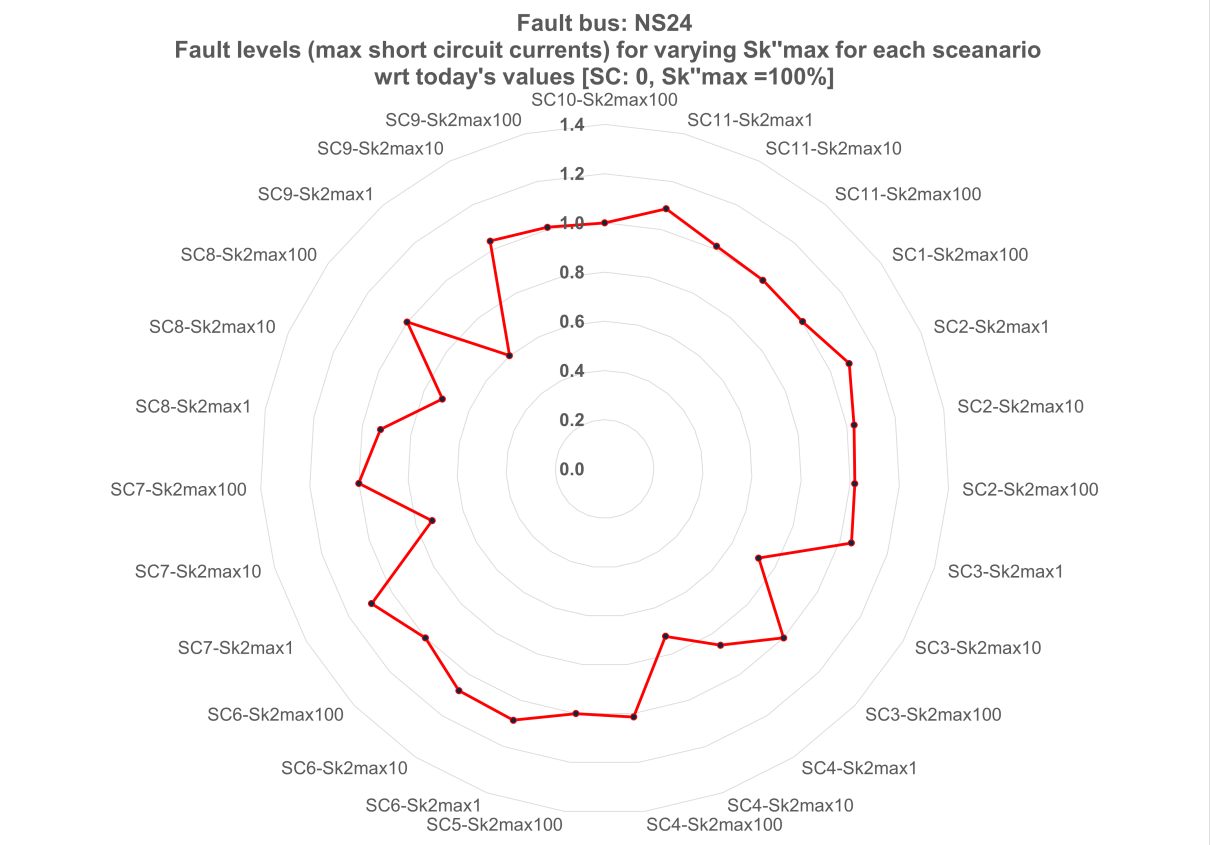


Figure 22: Maximum short-circuit currents, $I_k^{''}$ for the LV node NS24 [**at the very end of Feeder 2**] for all combinations of $S_{k-max}^{''}$ for each scenario (SC1-SC11) with respect to the today's value (1.0) for the base-case scenario, SC0 and $S_{k-max}^{''} = 100\%$

## 3.3 RMS results: Maximum short-circuit currents through MV-LV transformers

Figures 23, 25 and 27 present the results of three transformers, strategically selected based on their proximity to the HV-MV substation. The results show the highest short-circuit currents flowing through each transformer for a given scenario, among $3\phi$ faults simulated at each node at a time. Note that, the results for today's conditions as the base-case scenario, SC0, with full availability of short-circuit current contribution from upper grids, $S_k^{''} = 100\%$ is denoted by green. As highlighted in Figure 9 the transformer 1522 is located at the very end of Feeder 2, while 1524 is located in very close proximity of HV-MV substation and 1526 is located in the middle of Feeder 1.

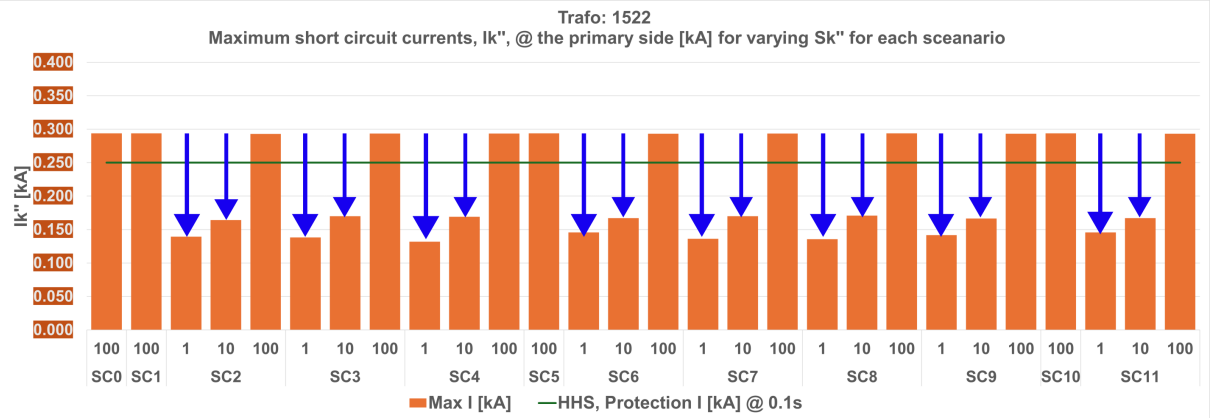


Figure 23: Using Method (i) : Maximum short-circuit currents, $I_k^{''}$ for the transformer 1522 [**at the very end of Feeder 2**] for all combinations of $S_{k-max}^{''}$ for each scenario (SC0-SC11) - Compare with Figure 24.

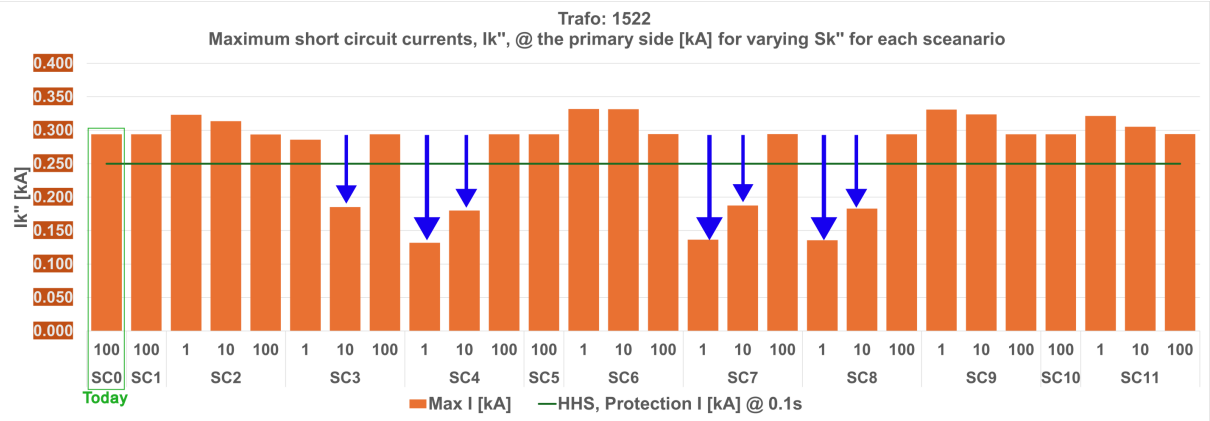


Figure 24: Using Method (ii) : Maximum short-circuit currents, $I_k^{''}$ for the transformer 1522 [**at the very end of Feeder 2**] for all combinations of $S_{k-max}^{''}$ for each scenario (SC0-SC11) - Compare with Figure 23.

The presented results in Figures 23, 25 and 27 are obtained by extracting the initial peak short-circuit current following the fault as described as Method (i) in Section 2.2. It is clearly observed that the reduction in the short-circuit contribution from upper grids, $S_k^{''}$, results in significant drops in the maximum short-circuit currents, $I_k^{''}$, which are lower than the protection settings and will cause delayed or non-activation of the protection devices. It is also observed that when the Method (ii) is used in Section 2.2, based on extracting the maximum value of the current during one cycle following the fault, the current contributions of some PVs are increasing further, especially in scenarios SC2, SC6, SC9 and SC11 and when the $S_k^{''}$ drops as shown in Figures 24, 26 and 28. This phenomenon is due to the response characteristics of the converter controls, which are not universal and depends on how they are tuned. Note that slight increase in short-circuit currents, with respect to the base-case, do not present a challenge to the existing protection layout.

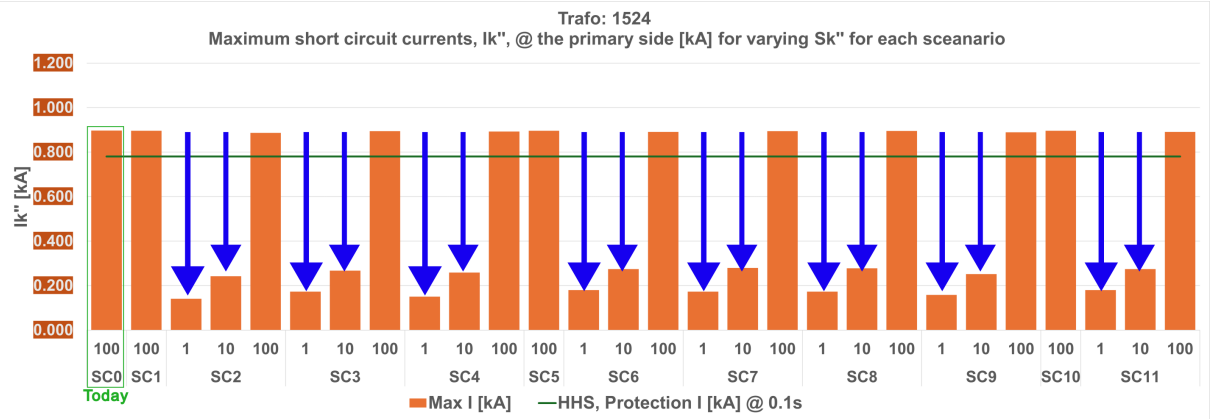


Figure 25: Using Method (i) : Maximum short-circuit currents, $I_k^{''}$ for the transformer 1524 [**close to the HV-MV transformer**] for all combinations of $S_{k-max}^{''}$ for each scenario (SC0-SC11) - Compare with Figure 26.

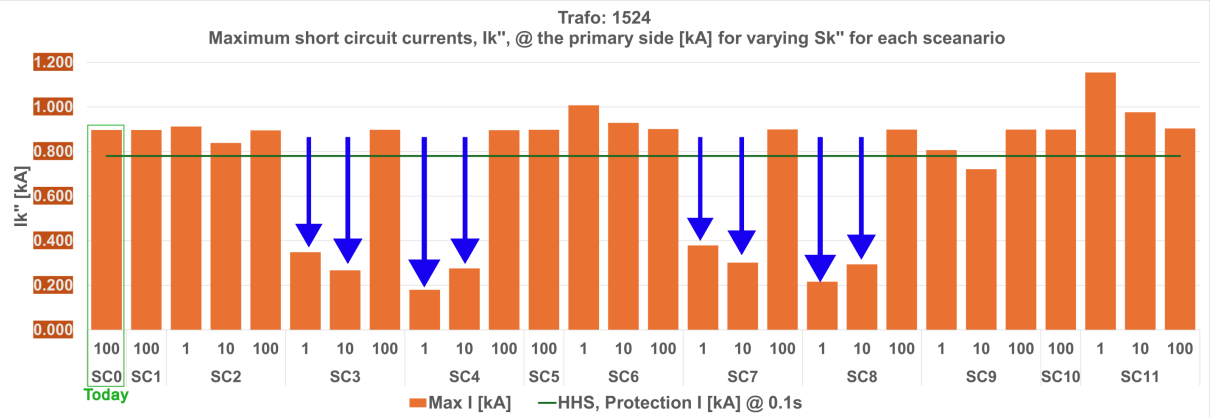


Figure 26: Using Method (ii) : Maximum short-circuit currents, $I_k^{''}$ for the transformer 1524 [**close to the HV-MV transformer**] for all combinations of $S_{k-max}^{''}$ for each scenario (SC0-SC11) - Compare with Figure 25.

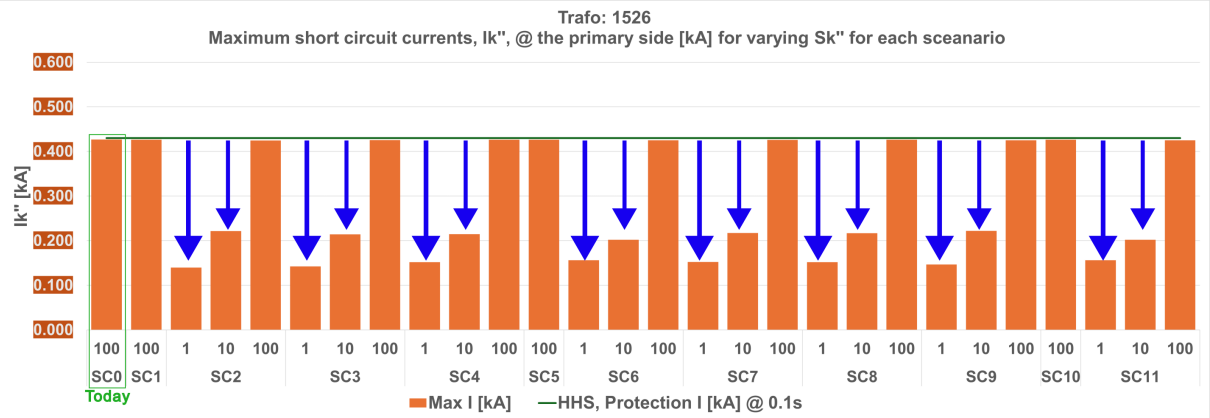


Figure 27: Using Method (i) : Maximum short-circuit currents, $I_k^{''}$ for the transformer 1526 [**in the middle of the Feeder 2**] for all combinations of $S_{k-max}^{''}$ for each scenario (SC0-SC11) - Compare with Figure 28.

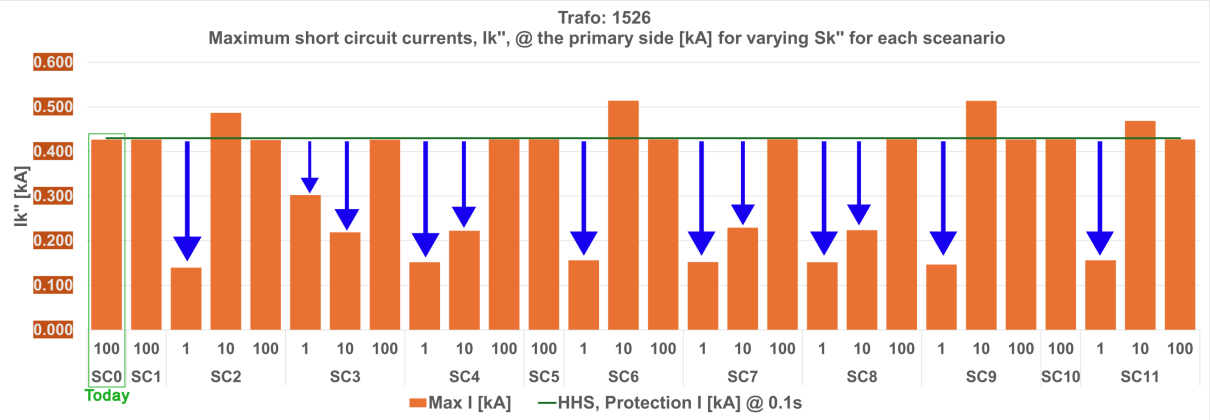


Figure 28: Using Method (ii): Maximum short-circuit currents, $I_k^{''}$ for the transformer 1526 [**in the middle of the Feeder 2**] for all combinations of $S_{k-max}^{''}$ for each scenario (SC0-SC11) - Compare with Figure 27.

## 3.4 RMS results: Maximum short-circuit currents through cables

The presented results in this section are based on the results of the Method (ii) , as described in Section 2.2, extracting the maximum value of the current during the one cycle following the fault. Figure 29 illustrates the maximum short-circuit currents flowing through the selected cables (in Feeder 1: 773, 787; in Feeder 2: 800, 805, 810, 795) as highlighted in Figure 9 for the base-case for a fault at the MV node MS23, which is located at the very end of the Feeder 2. As expected, the short-circuit current flowing through the cables 800, 805 and 810 is same, as they are in series, provided by the upper grids. The protection and the back-up protection illustrated in Figure 10 are designed according to this operation, when the conventional generators in EHV/HV grids are the only sources of the short-circuit currents for faults in MV and LV grids. As expected, the short-circuit currents flowing through the cables in Feeder 1 are insignificant.

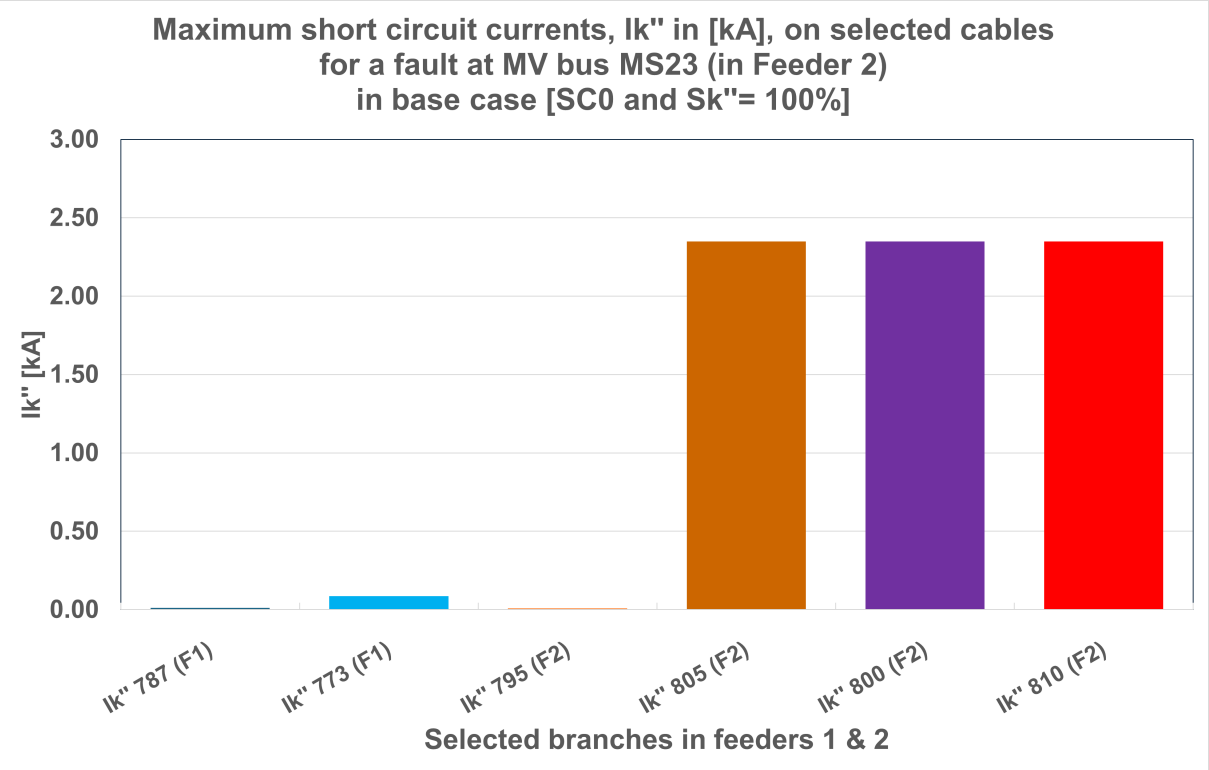


Figure 29: Maximum short circuit currents, $I_k''$ in [kA] on selected cables in Feeders 1 & 2 for a fault at MV bus MS23 in **Feeder 2** in base-case (SC0) & $S_k'' = 100\%$

Figure 30 illustrates the results for maximum short circuit currents, $I_k''$, for the same fault at the same bus (MS23) in all scenarios with high proliferation of distributed generation, when the short-circuit current contribution from upper grids, $S_k'' = 100\%$, i.e., at today's levels. Note that, the short-circuit currents flowing through the cables in Feeder 2 are not significantly affected, however, as indicated by green dashed rectangles, significant short-circuit currents are observed on cable 773 in Feeder 1, due to the short-circuit current contribution by distributed generation located in Feeder 1. This phenomenon can cause unnecessary tripping in Feeder 1 if the protection devices are directional and not blocking the upstream short-circuit currents and illustrates the "nuisance & sympathetic tripping" problem as explained in Section 2.

Figure 31 presents the results for maximum short circuit currents, $I_k''$, for the same fault at the same bus (MS23) in all scenarios with high proliferation of distributed generation, when the short-circuit current contribution from upper grids, $S_k''$ significantly drops to $10\%$ of today's levels. The significant drop in maximum short circuit currents are observable in all scenarios with PVs indicated by green dashed rectangle, which will result in delayed or non-activation of the protection devices. This phenomenon is referred to as "protection under-reach" as explained in Section 2. In addition, as indicated by green dashed lines, the maximum short-circuit current levels along the cables are different due to short-circuit contributions by DGs, which affects the back-up coordination among the protection devices, rendering the need for re-setting the back-up coordination. For the sake of completeness, the results for a $3\phi$ fault

at MV node MS11 in Feeder 1 are also provided similarly in Figure 32, 33 and 34.

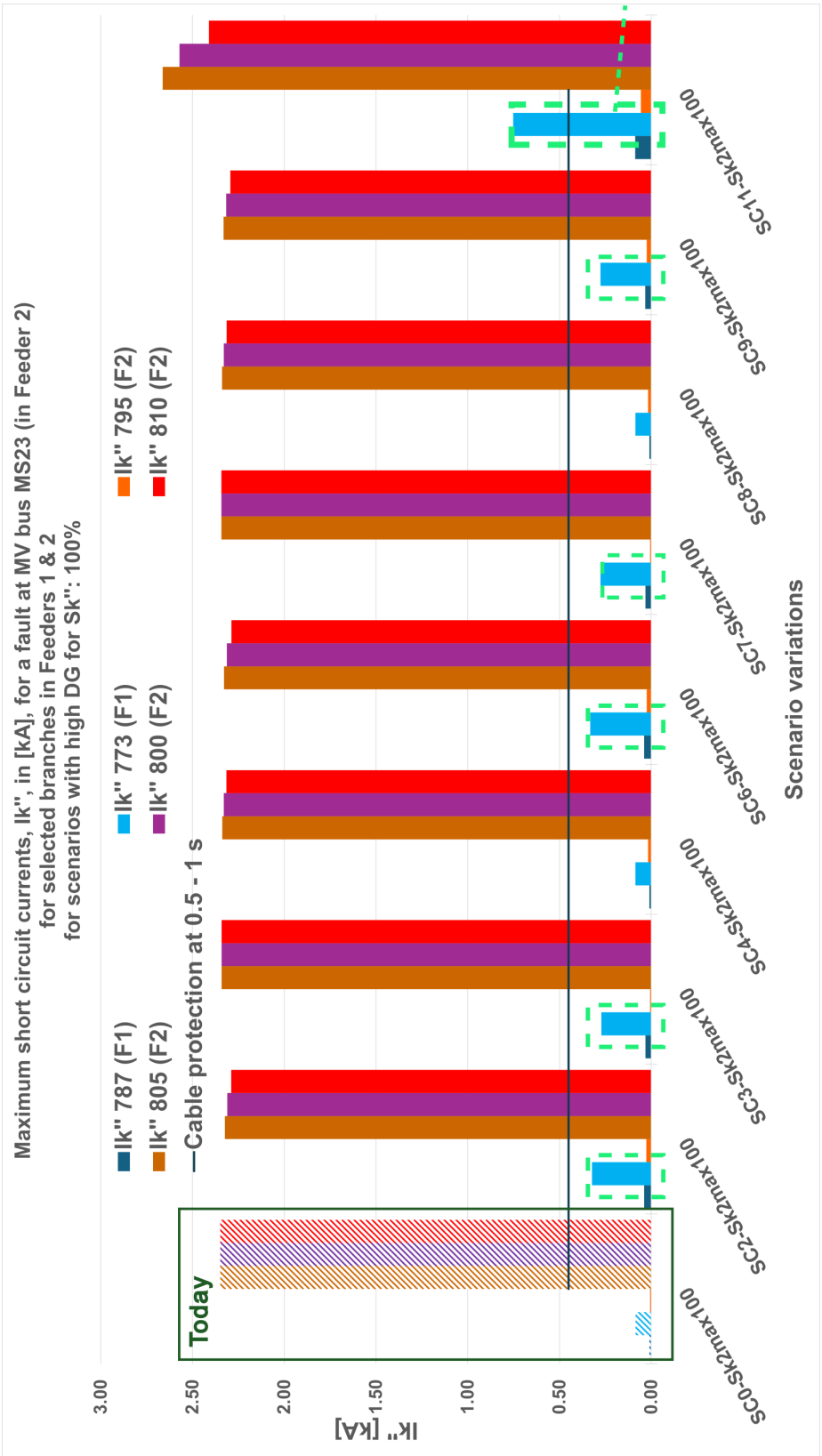


Figure 30: Maximum short circuit currents, $I_k''$ in [kA] on selected cables in Feeders 1 & 2 for a $3\phi$ fault at MV bus MS23 in **Feeder 2** in all scenarios with high distributed generation for $S_k'' = 100\%$

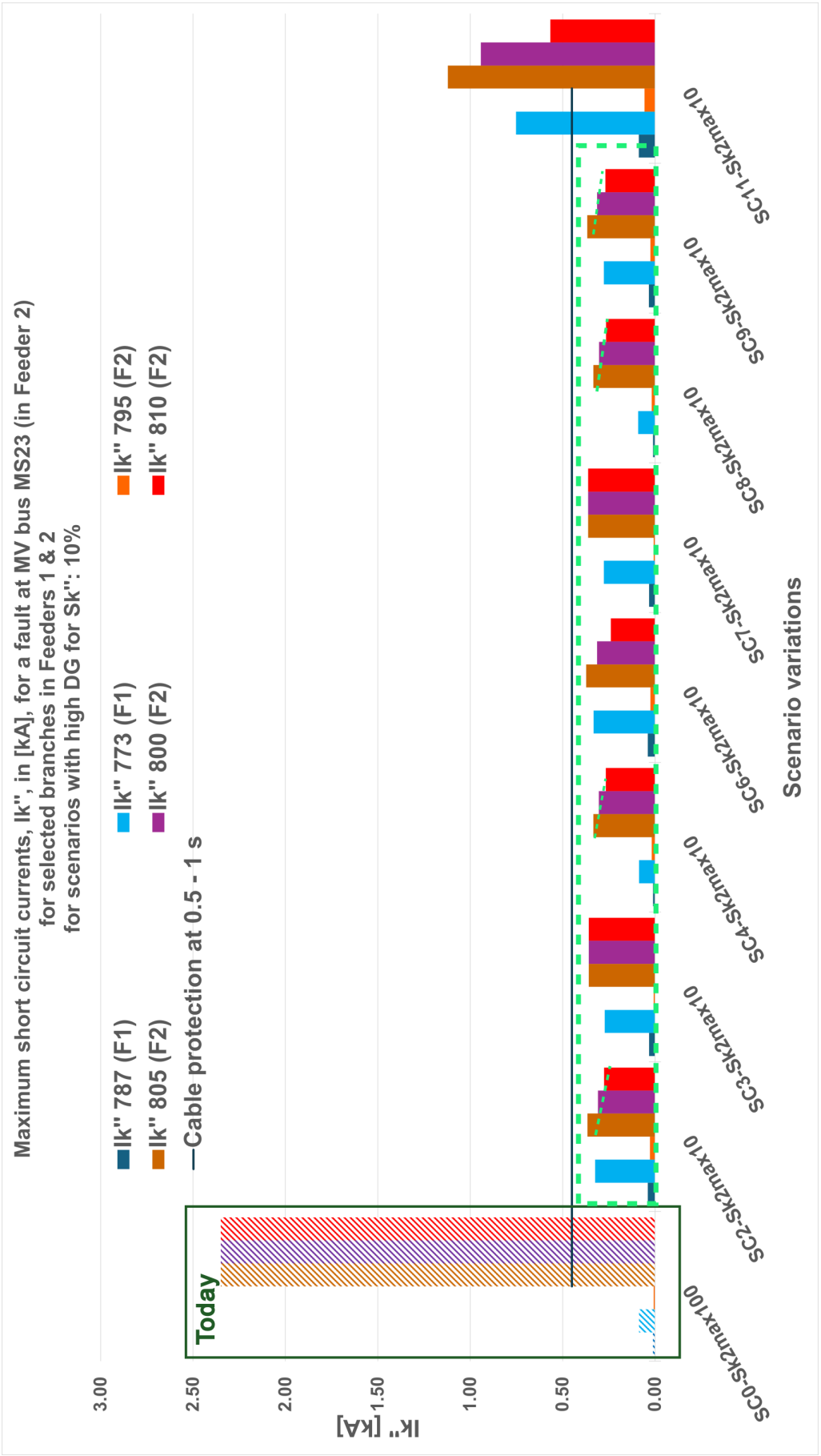


Figure 31: Maximum short circuit currents, $I_k''$ in [kA] on selected cables in Feeders 1 & 2 for a fault at MV bus MS23 in **Feeder 2** in all scenarios with high distributed generation for $S_k'' = 10\%$

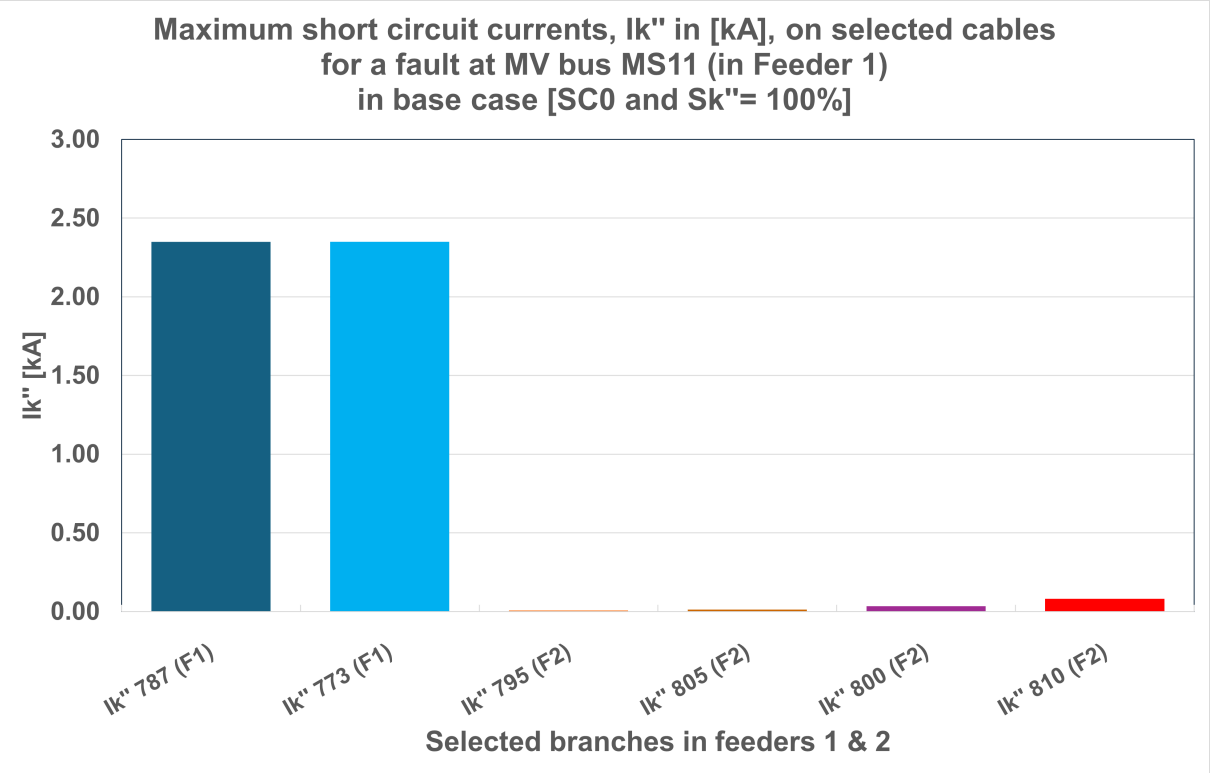


Figure 32: Maximum short circuit currents, $I_k''$ in [kA] on selected cables in Feeders 1 & 2 for a fault at MV bus MS11 in **Feeder 1** in base-case (SC0) & $S_k'' = 100\%$

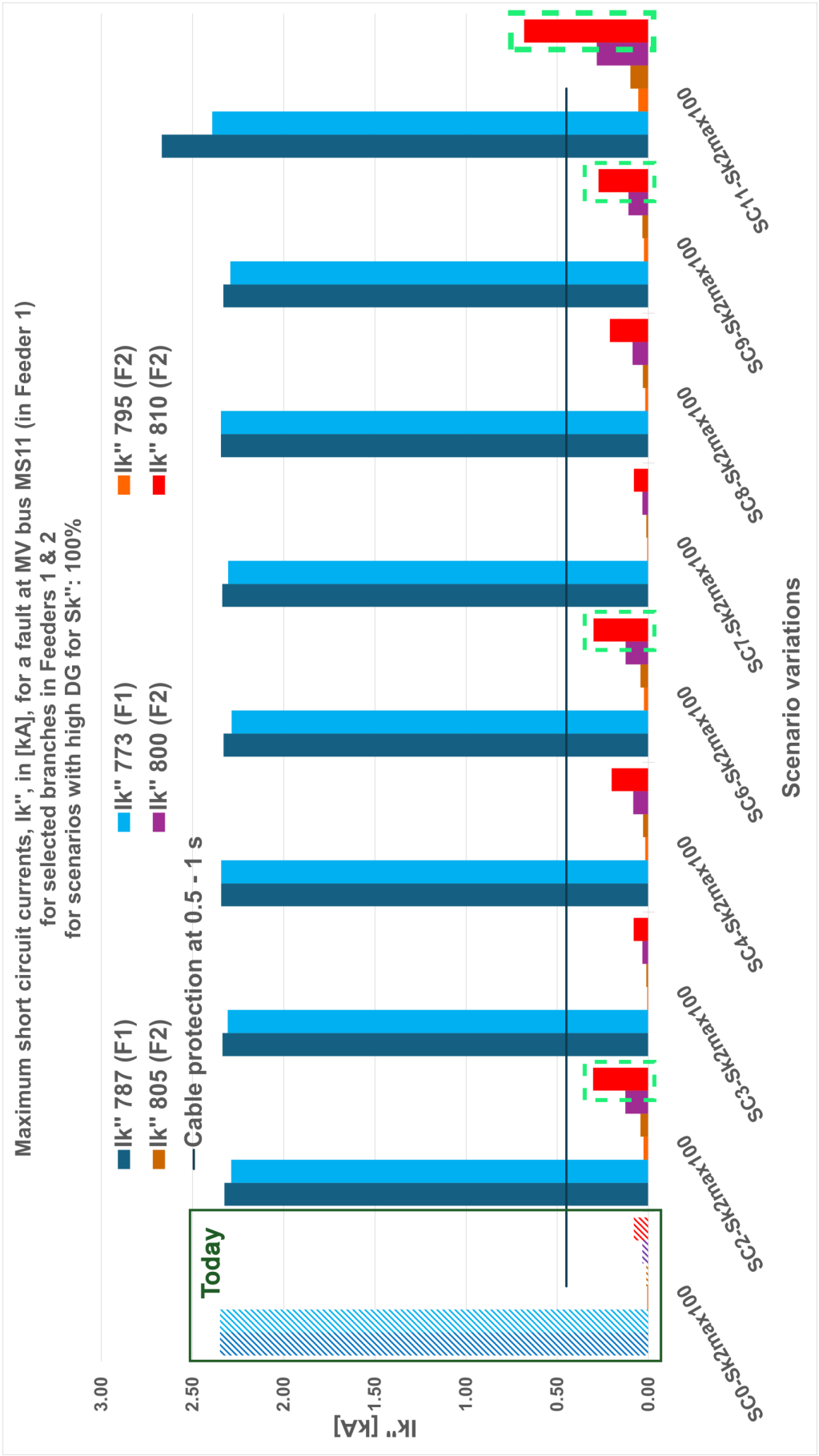


Figure 33: Maximum short circuit currents, $I_k''$ in [kA] on selected cables in Feeders 1 & 2 for a fault at MV bus MS11 in **Feeder 1** in all scenarios with high distributed generation for $S_k'' = 100\%$

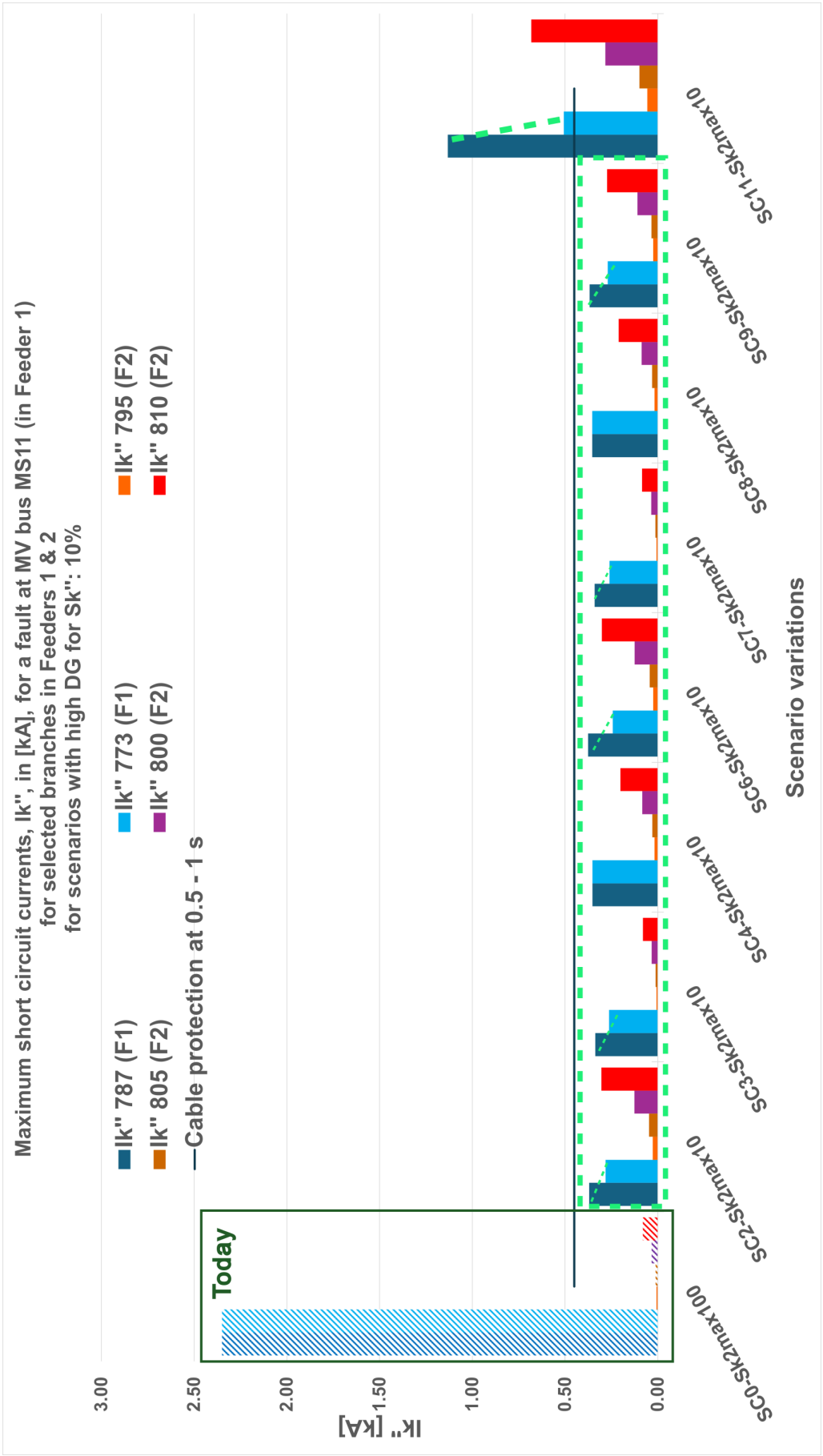


Figure 34: Maximum short circuit currents, $I_k''$ in [kA] on selected cables in Feeders 1 & 2 for a fault at MV bus MS11 in **Feeder 1** in all scenarios with high distributed generation for $S_k'' = 10\%$

# 4 Conclusions

In this report, the benefits of **RMS** simulations (compared to the results of the IEC60909-2016 standard) for protection studies are demonstrated. For RMS simulations, the FEN in-house tool, **FlexDYN**, is used. Following, the fault levels (i.e., short-circuit current levels, $Ik''$) in a given MV grid for selected grid operating states with high and low renewable energy resources such as PV is assessed. The impacts of different fault levels in selected grid operating states on overcurrent protection of MV-LV transformers and MV cables as well as back-up protection are demonstrated, and finally a non-exhaustive list of potential mitigation measures are provided. The **following conclusions** are drawn based on the simulations and analyses, using an MV grid, shared by EKZ in PowerFactory format, including MV-LV transformers, while the LV loads are aggregated at the LV side of the transformers.

1. It is essential to consider the time-variant short-circuit current (i.e., fault level, $S_k''$) contribution from upper grids, projected for 2035+ when the number of spinning generators will be daily and seasonally changing in the ENTSO-E region.
2. As $S_k''$ decreases to 10% of today's value (implying that the short-circuit contribution of EHV decreases due to fewer number of online rotating machines),
    - the differences between RMS and IEC6090 results are significant,
    - the fault levels decrease such that the present overcurrent protection devices may not detect the faults within the present time settings. This phenomena is observable only with the RMS simulations.
3. Using RMS or EMT simulations provide better insight for analyzing the short-circuit phenomena compared to the calculations based on IEC60909-2016 standard because
    - it is difficult to estimate the inverter impedances: Converters do not have universal short-circuit response characteristics, and
    - RMS and EMT simulations consider inherently the actual nodal voltages (pre-fault & during-fault) in the system rather than relying on assumptions in IEC60909 based on nominal voltages (1 p.u.)
4. IEC60909-2016 may significantly underestimate or overestimate the fault level at the LV bus depending on (i) the location of the LV bus (i.e., proximity to HV-MV transformer), (ii) the MV-LV transformer's characteristics, and (iii) the location of the PVs (i.e., at MV vs. LV).
5. Increase in maximum short-circuit currents is observed but not expected to affect the protection functionalities
6. Decrease in maximum short-circuit currents (e.g., on a Summer day at 12:00) due to a reduction in contribution from upper grid levels, will cause "**protection under-reach**": not activation or delayed activation of protection devices
    - affecting the lifetime of affected equipment such as cables due to longer-than-expected exposure to stress
    - affecting the voltage quality due to sustained voltage sags
    - not-cleared "permanent" faults presents danger for human life
    - eventually risking an increase in the system reliability index, SAIDI, (system average interruption duration index)
7. Due to short-circuit current contribution of solar PVs, unnecessary activation of protection devices in feeders without faults are expected if the protection devices are nondirectional, resulting in "**nuisance & sympathetic tripping**"
    - causing unnecessary interruption of the service
    - increasing the system reliability index, SAIDI
8. Due to short-circuit current contribution of solar PVs, the protection back-up coordination for overcurrent protection of cables are expected to be severely affected

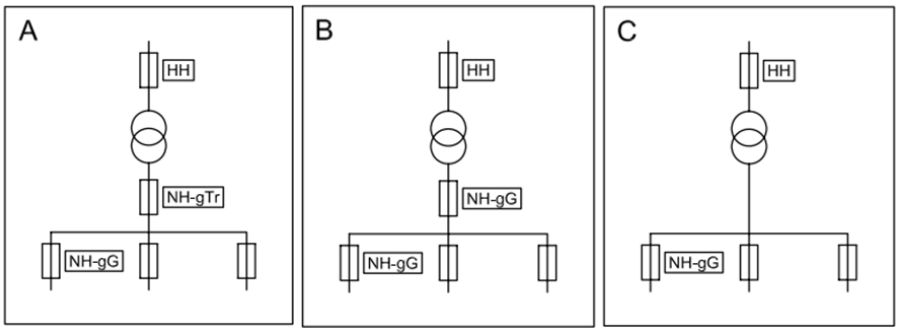


Figure 35: Various protection and protection coordination layouts. Courtesy of SIBA HV-fuse catalog

- causing delayed activation or not activation of the back-up protection device in case of failure of a protection device

9. The short-circuit current levels at the low voltage side of the transformers are expected to be affected. If the utility uses HHS (Hochspannungs-Hochleistungs-Sicherung / HV-fuse) in coordination with the protection devices at the LV feeders (see Figure 35 for three examples), the coordination settings shall be re-assessed.

Following is a non-exhaustive list for **candidate mitigation measures**. Note that these are technically feasible solutions, and some may not be economical for all MV grids. Assessing the economic feasibility is not within the scope of this project.

1. Grid technology oriented:
   - Employ rotating machine-driven renewable energy resources (e.g., biogas, biomass, geothermal) at MV grids, as spinning reserves (online but not producing).
   - Deploying synchronous condensers at EHV/HV or at MV grids at strategic locations. These machines are mainly used for ”dynamic” voltage support by flexibly providing or consuming reactive power, and can supply short-circuit current during faults.
   - Deploying STATCOM-BESS solutions at MV grids, which are designed to provide the same services provided by synchronous condensers.
2. Protection device oriented:
   - Use adaptive setting banks for overcurrent protection and back-up coordination based on the seasons and time-intervals in a day (e.g., at least two settings on a Summer day),
   - Deploy non-directional overcurrent protection along MV feeders or at strategic locations to prevent the short-circuit contributions of solar PVs.
   - Use distance protection at both sides of selected MV segments, similar to the implementation in EHV/HV grids, and rely on impedance estimation based on measured voltage and currents (rather than relying only on voltage measurements with overcurrent relays or fuses).
   - Use differential protection for selected MV segments.
3. Converter oriented:
   - Require the solar PVs to provide negative sequence short-circuit current contribution.

# 5 Suggestions for future research

**For EHV/HV grid operators (e.g., Swissgrid, Axpo)**:

- A fault level assessment for the Swiss EHV/HV grids is necessary for 2035 and beyond, considering the reduction in available short-circuit current contribution through inter-ties between neighboring countries. Such analysis would require a reliably accurate model of the European energy market to identify the generation layout at selected operational instants.

**For DSOs**:

- PV hosting capacity analyses in MV and LV grids shall be performed or at least assessed from the perspective of protection layouts, and the proliferation of converter-interfaced sources have to be closely monitored and steered accordingly so that problems such as ”**protection back-up coordination**” and ”**nuisance & sympathetic tripping**” are avoided. A Swiss-wide guideline for PV hosting capacity analysis in MV-LV grids taking into account the protection perspective would be beneficial to the industry, especially focusing on a set of projected problems for currently most common protection layouts.
- Simulating (RMS/EMT) and investigating MV and LV networks together will provide more insights to the evolution of short-circuit currents and their impacts on the protection layouts.
- Including the feeder reconfiguration (e.g., N-1 setup in MV) in the scenarios to assess the protection layout is very important.
- Analysis of MV grids with different characteristics such as rural, urban, semi-rural, elongated, covering a large area will provide insights to the level of impact.

**For converters**:

- A P&D project focusing on the testing of the widely-used PV converters in Switzerland to assess their short-circuit contribution behavior would be insightful for the industry, with consideration of the grid code for internal NA-EEA protection.
- Understanding the short-circuit behavior of the grid forming converters and their impacts on the protection layout is important.
- Understanding the short-circuit response of various heat pump technologies by means of a P&D project would be insightful for the industry.

# 6 Acknowledgement

We would like to thank Dr. Marina Gonzalez Vaya, Tam Nguyen Thi Thanh, Christoph Schaedeli, Dr. Julian Wruk at EKZ for providing the MV grid, for fruitful discussions and valuable feedback.

# 7 References

[1] S. M. Brahma and A. A. Girgis. Development of adaptive protection scheme for distribution systems with high penetration of distributed generation. *IEEE Transactions on Power Delivery*, 19(1):56–63, Jan 2004.

[2] C. Y. Evrenosoglu and A. Abur. Fault location in distribution systems with distributed generation. In *The 15th Power Systems Computation Conference Liege,*, pages 384–388, August 2005.

[3] N. Perera, A. D. Rajapakse, and T. E. Buchholzer. Isolation of faults in distribution networks with distributed generators. *IEEE Transactions on Power Delivery*, 23(4):2347–2355, 2008.

[4] S. M. Brahma. Fault location in power distribution system with penetration of distributed generation. *IEEE Transactions on Power Delivery*, 26(3):1545–1553, July 2011.

[5] B. Hussain, S. M. Sharkh, S. Hussain, and M. A. Abusara. An adaptive relaying scheme for fuse saving in distribution networks with distributed generation. *IEEE Transactions on Power Delivery*, 28(2):669–677, 2013.

[6] S. F. Alwash, V. K. Ramachandaramurthy, and N. Mithulananthan. Fault-location scheme for power distribution system with distributed generation. *IEEE Transactions on Power Delivery*, 30(3):1187–1195, 2015.

[7] M. J. Reno, R. J. Broderick, J. Seuss and S. Grijalva, “Determining the Impact of Steady-State PV Fault Current Injections on Distribution Protection,” SANDIA National Laboratories Report, 2016.

[8] International Electrotechnical Commission, “IEC 60909-0 Short-circuit current in three-phase a.c. systems - Part 0 Calculation of currents,” International Standard [DIN EN 60909-0 (VDE 0102):2016-12], 2016.

[9] I. Kasikci. *Short Circuits in Power Systems: A practical guide to IEC60909-0 2nd edition*. Wiley, 2018.

[10] M. Plenz, F. Grumm, M. F. Meyer, S. Boden, D. Schulz, and K. Lehmann. Szenariobasierte analyse der kurzschlussströme im deutschen niederspannungsnetz unter verwendung der cigre-referenznetze. *Elektrotechnik and Informationstechnik*, 138(4-5):289–299, 2021.

[11] R. Schürhuber. Die kurzschlussnorm iec 60909-0: 2016– neues und Änderungen. *Elektrotechnik and Informationstechnik*, 133(4-5):228–235, 2016.

[12] R.M. Furlaneto, I. Kocar, A. Grilo-Pavani, U. Karaagac, A. Haddadi, and E. Farantatos. Short circuit network equivalents of systems with inverter-based resources. *Electric Power Systems Research*, 199:107314, 2021.

[13] Insu Kim. Short-circuit analysis models for unbalanced inverter-based distributed generation sources and loads. *IEEE Transactions on Power Systems*, 34(5):3515–3526, 2019.

[14] IEEE/NERC Task Force on Short-Circuit and System Performance Impact of Inverter Based Generation, “Impact of Inverter Based Generation on Bulk Power System Dynamics and Short-Circuit Performance,” IEEE PES Technical Report National Laboratories Report PES-TR68, 2018.

[15] F. Katiraei, J. Holbach, T. Chang, W. Johnson, D. Wills, B. Young, L Marti, A. Yan, P Baroutis, G. Thompson, and J Rajda. Investigation of solar pv inverters current contributions during faults on distribution and transmission systems interruption capacity. In *Western Protective Relay Conference*, pages 1–5, Oct. 2012.

[16] R. Aljarrah, H. Marzooghi, J. Yu, and V. Terzija. Monitoring of fault level in future grid scenarios with high penetration of power electronics-based renewable generation. *IET Generation, Transmission & Distribution*, 15(2):294–305, 2021.

[17] International Electrotechnical Commission, “IEC 60076-5 Power transformers - Part 5: Ability to withstand short circuit,” International Standard, 2006.

[18] RWTH Aachen. "Studie zu Aspekten der elektrischen Systemstabilität im deutschen Übertragungsnetz bis 2023," Bundesnetzagentur BNETZA Final Report, 2015.

[19] NREL National Renewable Energy Laboratory. Understanding fault characteristics of inverter-based distributed energy resources, 2010.

[20] H. Ravindra, M. O. Faruque, P. McLaren, K. Schoder, M. Steurer, and R. Meeker. Impact of pv on distribution protection system. In *2012 North American Power Symposium (NAPS)*, pages 1–6, 2012.

[21] L. Steinhaeuser, M. Coumont, S. Weck, and J. Hanson. Comparison of rms and emt models of converter-interfaced distributed generation units regarding analysis of short-term voltage stability. In *NEIS 2019; Conference on Sustainable Energy Supply and Energy Storage Systems*, 2019.

[22] "Larsson M., A. Fuchs, and T. Demiray. "ACSICON: Novel Analysis and Control Solutions for Dynamic Security Issues in the Future," Swiss Office of Energy SFOE Final Report SI/501728, 2021.

[23] T. Demiray, F. Milano, and G. Andersson. Dynamic phasor modeling of the doubly-fed induction generator under unbalanced conditions. In *2007 IEEE Lausanne Power Tech*, pages 1049–1054, 2007.

[24] T. Demiray, G. Andersson, and L. Busarello. Evaluation study for the simulation of power system transients using dynamic phasor models. In *IEEE/PES Transmission and Distribution Conference and Exposition: Latin America*, pages 1–6, 2008.

[25] Turhan Demiray. *Simulation of power system dynamics using dynamic phasor models*. PhD thesis, ETH Zurich, 2008.

[26] Alexander Fuchs, Turhan Demiray, and Mats Larsson. Aggregated models of active distribution networks for stability studies of large transmission systems. *Electric Power Systems Research*, 212:108607, 2022.

[27] A. Kubis, S. Rüberg and C. Rehtanz, “Development of available short-circuit power in Germany from 2011 up to 2033,” CIRED Workshop Rome, 2014.

[28] Australian Energy Market Operator, “Short-circuit levels for the Victorian electricity transmission network,” 2016.

[29] Western Power Distribution UK, “FlexDGrid: Advanced fault level management in Birmingham,” Closedown Report, 2017.

[30] New York Independent System Operator, “NYISO Fault current assessment,” Report, 2017.

[31] National Grid (UK), “Electricity Ten Year Statement 2019: Appendix D: Fault level narrative and data,” 2019.

[32] S. Boljevic and M. F. Conlon. Fault current level issues for urban distribution network with high penetration of distributed generation. In *2009 6th International Conference on the European Energy Market*, pages 1–6, May 2009.

[33] P. Karaliolios, A. Ishchenko, E. Coster, J. Myrzik, and W. Kling. Overview of short-circuit contribution of various distributed generators on the distribution network. In *2008 43rd International Universities Power Engineering Conference*, pages 1–6, Sep. 2008.

[34] Salvatore D’Arco, Jon Are Suul, and Olav B. Fosso. A virtual synchronous machine implementation for distributed control of power converters in smartgrids. *Electric Power Systems Research*, 122:180–197, 2015.